



UNIVERSITÀ DEGLI STUDI DI PADOVA

DIPARTIMENTO DI TECNICA E GESTIONE DEI SISTEMI INDUSTRIALI
CORSO DI LAUREA TRIENNALE IN INGEGNERIA MECCANICA E
MECCATRONICA - CURR. MECCATRONICO

TESI DI LAUREA TRIENNALE

**STUDIO DI FATTIBILITÀ DI UNA FRIZIONE A
COMANDO ELETTRICO PER UN VEICOLO
FSAE**

**Progettazione e considerazioni
sull'implementazione**

Relatore: Prof. Mauro Zigliotto

Laureando: Marco Zorzi
1004556

ANNO ACCADEMICO: 2013-14

To my fellow adventurers
of the Race UP Team.

Keep Pushing!

SUMMARY

The aim of this thesis is to discuss about the studies done to design the best configuration of an electric-actuated clutch of the MGo914 vehicle of the Race UP Team, the Formula SAE team of the University of Padova.

Formula SAE is a worldwide competition held among students and it challenges students to design, build and test a single seater racing car. The car is required to have performance, reliability as well as safety and low manufacturing and repairing costs. This requirements are described in a official set of rules which restricts numerous aspects of the vehicle, from the chassis to the engine and to other components. Nevertheless, these rules are permissive enough to let students to be creative and to have their imagination challenged.

In this script the gear change system previously adopted will be analyzed as a first step and, after that, design and calculation will be done, with particular focus on sizes of electrical actuators and their controls. In addition, the transmission system will be analyzed. In conclusion, the different solutions found will be compared in terms of costs, weights, performance and reliability.

CONTENTS

1	INTRODUCTION	1
1.1	Analysis of the previous solutions	1
1.2	Design motivations	3
2	MECHANICAL SYSTEM ANALYSIS	5
2.1	Mechanical system description	5
2.2	Working parameters calculation	6
2.2.1	Speed requirements	6
2.2.2	Torque requirements	8
2.3	Torque requirements experiments	10
2.3.1	Hang masses	10
2.3.2	Structure with torque wrench	11
2.4	Transmission system	13
2.4.1	Motor connected axially to the clutch vertical shaft	13
2.4.2	Motor with cylinder and cable	13
2.4.3	Ball screw	14
3	STEPPER MOTOR SIZING	17
3.1	Stepper Motors - introduction	17
3.1.1	Switched reluctance motors	17
3.1.2	Permanent magnet motors	18
3.1.3	Hybrid stepping motors	19
3.2	Stepper Motor sizing	20
3.2.1	Anaheim Automation 34K314S-LW8	21
3.2.2	Anaheim Automation 34K112S-LW8	24
3.2.3	Anaheim Automation 24Y504S-LW8	27
3.2.4	Anaheim Automation 24Y508S-LW8	31
3.2.5	Applied Motion HT34-504	34
3.2.6	Comparison	37
3.3	MATLAB® Simulation	37
3.3.1	Linear speed vs time	38
3.3.2	Angular speed vs time	38
3.3.3	Angular speed in pps vs time	38
3.3.4	Torque required vs time	40
3.3.5	Torque required vs speed	40
3.3.6	Torque required and pullout torque vs speed	41
3.3.7	Commutation period	42
4	BRUSHLESS DC MOTOR SIZING	43
4.1	Brushless DC Motors - introduction	43
4.1.1	Structure	44
4.1.2	Working Principle	44
4.2	Revised transmission system	45
4.3	BLDCM Motor sizing	46

4.3.1	Thermal model	46
4.3.2	Matlab scripts	49
4.3.3	Faulhaber 3056 K 012 B	50
4.3.4	Faulhaber 2057 S 012 B	52
4.3.5	Faulhaber 3564 K 012 B	54
4.3.6	Maxon Motor EC-max 30 40 Watt	56
4.3.7	Maxon Motor EC-i 40 50 Watt	58
4.3.8	Maxon Motor EC-max 30 60 Watt	60
5	CONCLUSION	63
A	APPENDIX A - MATLAB®	65
B	APPENDIX B - MG0914 DATA ACQUISITION SYSTEM	67
C	APPENDIX C - MATLAB® SCRIPT BLDCM RATIO	69
D	APPENDIX D - MATLAB® SCRIPT BLDCM SIMULATION	71
	BIBLIOGRAPHY	73

LIST OF FIGURES

Figure 1	Mechanical clutch lever of MGo813	2
Figure 2	Technical drawing of the clutch system of Honda CBR600RR engine	5
Figure 3	Angle measurement extracted from two pictures overlapped	6
Figure 4	Desired law of motion and average speed	8
Figure 5	Masses hanged to the engine clutch lever	10
Figure 6	Total weight	10
Figure 7	Structure scheme for the maximum force calculation	11
Figure 8	Structure for the force calculation	12
Figure 9	Structure for the force calculation	13
Figure 10	SKF Catalogue	15
Figure 11	Switched reluctance motor operating principle [4]	18
Figure 12	Permanent magnet motors [2]	18
Figure 13	Side view and cross-sections of a hybrid stepping motor [2]	19
Figure 14	Static calculations with ball screw	21
Figure 15	Anaheim Automation 34K314S-LW8 total power calculations	22
Figure 16	Anaheim Automation 34K314S-LW8 torque required vs right hand lead	22
Figure 17	Anaheim Automation 34K314S-LW8 and required power comparison	23
Figure 18	Anaheim Automation 34K112S-LW8 total power calculations	25
Figure 19	Anaheim Automation 34K112S-LW8 torque required vs right hand lead	25
Figure 20	Anaheim Automation 34K112S-LW8 and required power comparison	26
Figure 21	Anaheim Automation 24Y504S-LW8 total power calculations	28
Figure 22	Anaheim Automation 24Y504S-LW8 torque required vs right hand lead	29
Figure 23	Anaheim Automation 24Y504S-LW8 and required power comparison	30
Figure 24	Anaheim Automation 24Y504S-LW8 total power calculations	31
Figure 25	Anaheim Automation 24Y504S-LW8 torque required vs right hand lead	32

Figure 26	Anaheim Automation 24Y504S-LW8 and required power comparison	33
Figure 27	Applied Motion HT304-504 total power calculations	34
Figure 28	Applied Motion HT304-504 torque required vs right hand lead	35
Figure 29	Applied Motion HT304-504 and required power comparison	36
Figure 30	Comparison of different motors	37
Figure 31	Desired linear law of speed	38
Figure 32	Desired speed law of speed for the motor	39
Figure 33	Desired speed law of speed for the motor expressed in sps	39
Figure 34	Torque required during the time of the movement	40
Figure 35	Torque required depending on the speed	41
Figure 36	Torque required compared with the pullout torque depending on the speed	41
Figure 37	Commutation periods to obtain the desired speed law	42
Figure 38	Structure of a Brushless DC Motor. (Courtesy of SERVO MAGNETICS INC, USA)	44
Figure 39	Working principle of a BLDCM Motor. [4]	45
Figure 40	Electrical-thermal model. Image courtesy of Maxon Motors.	48
Figure 41	Graphical user interface used for the Matlab scripts.	49
Figure 42	Peak temperature vs ratio.	51
Figure 43	Temperature raise vs time. Ratio 650.	51
Figure 44	Peak temperature vs ratio.	52
Figure 45	Temperature raise vs time. Ratio 1050	53
Figure 46	Peak temperature vs ratio.	54
Figure 47	Temperature raise vs time. Ratio = 400.	55
Figure 48	Temperature raise vs time. Ratio = 150	55
Figure 49	Peak temperature vs ratio.	56
Figure 50	Temperature raise vs time. Ratio 700.	57
Figure 51	Temperature raise vs time. Ratio 275.	57
Figure 52	Peak temperature vs ratio.	58
Figure 53	Temperature raise vs time. Ratio 700.	59
Figure 54	Temperature raise vs time. Ratio 285.	59
Figure 55	Peak temperature vs ratio.	60
Figure 56	Temperature raise vs time.	61
Figure 57	Temperature raise vs time.	61

Figure 58 Example of i2 Pro Data Acquisition software. 68

INTRODUCTION

1.1 ANALYSIS OF THE PREVIOUS SOLUTIONS

During the various developments of Race UP Team's prototypes, since the gear shift is done without using the clutch, the clutch itself and its actuation have always been considered of secondary importance. As a consequence, from the first to the last prototype, there was an evolution of the system from a clutch pedal, as commonly done in every vehicle, to a clutch lever, firstly positioned fixed to the steering boss and, later on, the clutch lever was designed to be on the side of the steering wheel with a precise position. These choices were made considering the weight reduction as first aim and led to a weight reduction and better handling without losing driver comfort. In the last team's car, the MGo813, the clutch lever was built with a "T" shape made with steel tubes (fig. 1); this lever, when pulled, allows the driver to pull the steel cable which is then linked to the engine clutch lever. A solution like the one just presented offers these advantages:

- It reduces the pedal box width and, as a consequence, the width of the front part of the chassis.
- It allows the driver to always have both feet on gas and brake pedals.
- Weight saving.
- Low costs.

Nevertheless, during various test sessions on track the car showed to be unreliable in the gear down shift, having issues in properly engaging the lower gear. From drivers feedback it was understood that these problems could be overcome by executing a so called "Throttle Blip": this is a well known technique in motorsport which is a rapid increase of the engine RPMs caused by the driver hitting the gas pedal for a short time. The "Throttle Blip" makes the engine RPMs to rise enough for the engaged gear to adapt to the speed of the lower gear and allowing the internal forks to shift the gear properly. Automatic blipping techniques are widespread in motorsport environment and they are usually made with small DC motors; this, unfortunately, is not allowed in the FSAE competitions because of the rule IC1.5.2:

IC1.5.2 Throttle Actuation

The throttle must be actuated mechanically, i.e. via a cable or a rod system. The use of electronic throttle control (ETC) or “throttle-by-wire” is prohibited.[3, p. 77]

An alternative to this technique, learnt from drivers' experience, is to slightly pull the clutch lever with the right hand, allowing a sure and reliable gear shift. Despite that, drivers have always defined this technique as distracting and tiring. The lever of the MGo813, being attached to the frame, forced drivers to remove the hand from the steering wheel and to pull the lever which, as it can be easily imagined, led to several disadvantages:

- A discrete amount of force is required to the driver.
- The driver must necessarily remove the hand from the steering wheel, causing safety risks.
- Being the vehicle without power steering or steer-by-wire (forbidden by the rules) it is quite hard to steer and particularly tiring so, adding the clutch lever can result in an excessive labour of the driver which would influence the overall performance.
- With the electric-pneumatic gear shift systems, it does not represent a reliable solution.



Figure 1: Mechanical clutch lever of MGo813

1.2 DESIGN MOTIVATIONS

During the numerous test sessions of the vehicle in order to improve its performance and reliability, a lot of care was put into the relationship between the car and the driver. A great importance was given to drivers' opinions aiming not only to improve the ergonomics of the vehicle but also to its features. As said before, there were issues with the down shift which forced the driver to use quite annoying techniques leading to loss of time, concentration, energies and performance.

As a result, two different solutions were considered to simplify the down shift task:

- Pneumatic system: Since the MGo813 is equipped with an high pressure air tank, the first idea was to design a pneumatic actuation with an electric air valve. By using this solution and controlling it with a PWM signal or with multiple air valves, a linear control of the force applied to the engine clutch lever could be achieved. Despite that, this solution requires to simulate the gas system in order to calculate the amount of gas needed for a specific amount of gear shifts and these calculations would require to assume data about the gas used which, as a matter of fact, is unknown. So, because of these uncertainties, it would be necessary to increase the overall size of the air tank in order to be sure and, by doing so, increasing the overall weight.
- Electric System: An electric actuator was the second hypothesis made. This solution would unlink the force required for the actuation of the engine clutch lever and the force actually required to the driver. As a result, this solution offers several advantages resulting in a totally autonomous system from the rest of the car and controllable through different control strategies and, if necessary, it could be easily adapted to be completely automatic. In addition, a self-made control system could permit to be easy customizable as well as flexible.

Since the electric solution seemed to offer more advantages it was chosen to deeply analyse different kinds of electric actuators and drives and, for each solution, to evaluate these parameters:

- Cost: being this design aimed to an actual realization, costs must be thoroughly considered by analysing the cost-benefits ratio.
- Weight: Another important requirement is to design the system to be as light as possible. Minimizing weights means lowering the total mass of the vehicle which leads to a lower rotational inertia and, so, to a better agility in turning.

- Control System: The control system must be the most economic and reliable possible. In addition, the difficulty of its implementation must be considered because, for cost reasons, self-made control systems are preferable.

As a consequence, it is necessary to correctly estimate the size of the electric drives in order to compare different solutions. To do this, experimental analysis had to be made in order to collect the necessary data. First of all, the transmission system was chosen among different kinds and, then, while sizing the electric drive, the precise model was defined.

MECHANICAL SYSTEM ANALYSIS

2.1 MECHANICAL SYSTEM DESCRIPTION

As shown in Figure 2, the Honda CBR600RR engine used in the vehicle is equipped with a clutch. The clutch movement starts with the force applied to a 37 mm length shaft which is outside the engine and which plays as interface between the mechanism and the user. The shaft is then connected to a perpendicular shaft which goes inside the engine and transforms the linear force exercised from the steel cable into a rotation of the second shaft. This vertical shaft acts on some cup springs and makes the friction discs to separate from each other, removing the friction and, so, the motion transmission. As a result, for the correct size estimation of the electric motor, it was necessary to find the required force to completely pull the engine clutch lever which corresponds to a torque required to the electric motor.

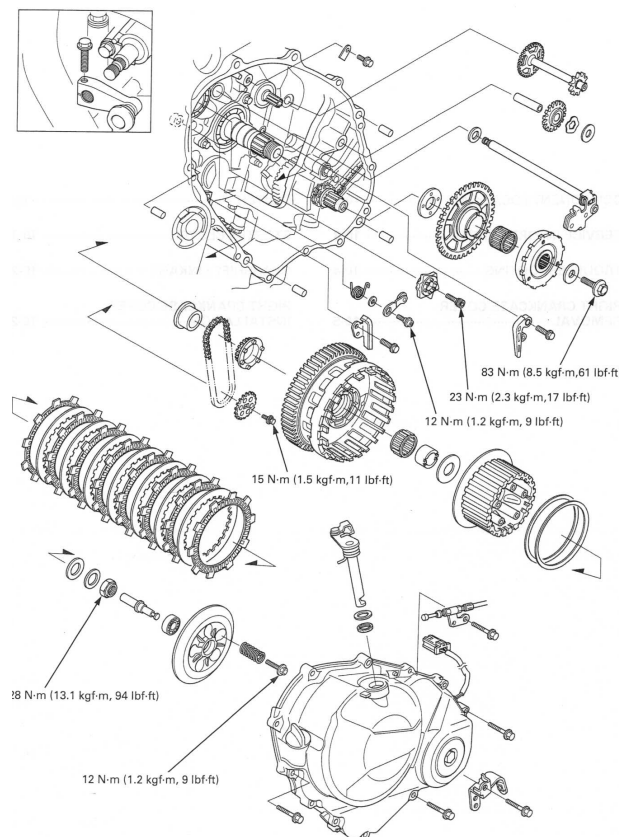


Figure 2: Technical drawing of the clutch system of Honda CBR600RR engine

2.2 WORKING PARAMETERES CALCULATION

To correctly estimate the size of an electric motor, the maximum torque and the maximum speed required to the motor must be known. In the following paragraphs these parameters will be analysed in detail.

2.2.1 *Speed requirements*

As said before, the MGo813 was equipped with an electric-pneumatic gear shift system controlled by the ECU (Engine Control Unit) which can change gear while cutting the engine power. For the up shift, the ECU operates cutting fuel injection and ignition for a total time of 150 ms. So, for the down shift, the maximum time permitted would be 250 ms because the car is supposed to be in a breaking phase and it is not required a too fast down shift. An ideal down shift would be around 100ms, which, as compared to 60-80 ms of F1 cars, is a quite good time. Unfortunately, during the design it was understood that the shift time deeply influences the final size and weight of the actuators and it is also difficult to find 12V actuators (which is the maximum voltage available on board). As a result, the motion time had to be risen to a maximum of 250ms. This time, even if more than the engine power cut time, it is enough for down shift 4 gears in 1 second.

In order to calculate the required speed, the angle of motion had to be found. As it can be observed in figure 3, with some photo editing software the angle of movement could be extracted and it resulted to be 34° .

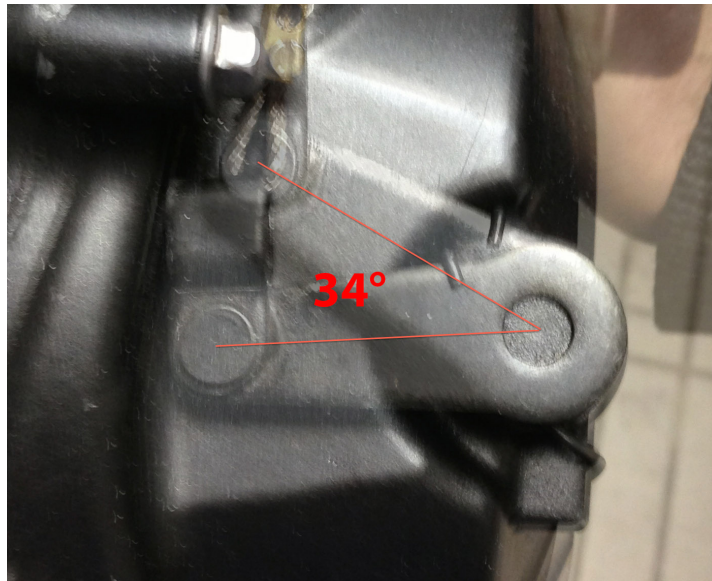


Figure 3: Angle measurement extracted from two pictures overlapped

From the hypothesis made, the average movement speed could be calculated using equation 1

$$\omega = \frac{d\theta}{dt} = \frac{0.5934\text{rad}}{0.25\text{s}} = 2.38\frac{\text{rad}}{\text{s}} \quad (1)$$

Then, from equation 2 the linear speed of the engine clutch lever could be calculated

$$v = \omega \cdot r = 2.38\frac{\text{rad}}{\text{s}} \cdot 0.037\text{m} = 0.088\frac{\text{m}}{\text{s}} \quad (2)$$

This value, anyway, is an average speed, which is ideal. In the real application, the motor would have to accelerate and decelerate, so a law of speed should be found in order to achieve an average speed of 0.088m/s. The law of speed was chosen to be a trapezoid shaped function with an average value of 0.088m/s. The rise and stop times were decided to be 20% the total time so to have a lower top speed but also a not excessive acceleration. This function is shown in figure 4.

The top speed was then calculated. Since a speed law was chosen, its integral is the position. By relating the integral to the area underneath the function, the top speed could be calculated as follows. During the calculations, this notation was used:

- A_{avg} = It is the area underneath the constant average speed.
- $\text{Speed}_{\text{avg}}$ = It is the average speed found in equation 2.
- Time_{tot} = Total time of motion, i.e. 250ms.
- $A_{\text{trapezoid}}$ = It is the area underneath the trapezoid shaped motion law.
- Time_{sp} = It stands for Time Speed Peak and it is the time in which the electric motor keeps the speed constant at the top speed.
- $\text{Speed}_{\text{peak}}$ = It is the maximum speed reached, the parameter to be calculated.

First, the area of the average speed motion is given by equation 3:

$$A_{\text{avg}} = \text{Speed}_{\text{avg}} \cdot \text{Time}_{\text{tot}} \quad (3)$$

Secondly, the area of the trapezoid speed motion law is given by equation 4:

$$A_{\text{trapezoid}} = \frac{\text{Time}_{\text{tot}} + \text{Time}_{\text{sp}}}{2} \cdot \text{Speed}_{\text{peak}} \quad (4)$$

So, since the electric drive must move for the same space, the two areas must be equals and by imposing

$$A_{\text{tot}} = A_{\text{trapezoid}} \quad (5)$$

and isolating $Speed_{peak}$ the result is

$$Speed_{peak} = 2 \cdot Speed_{avg} \cdot \frac{Time_{tot}}{Time_{tot} + Time_{sp}} \quad (6)$$

But, being

$$Time_{sp} = Time_{tot} - 2 \cdot Time_{rise} \quad (7)$$

Equation number 6 could be written as

$$Speed_{peak} = \frac{Speed_{avg} \cdot Time_{tot}}{Time_{tot} - Time_{sp}} = 0.11 \frac{m}{s} \quad (8)$$

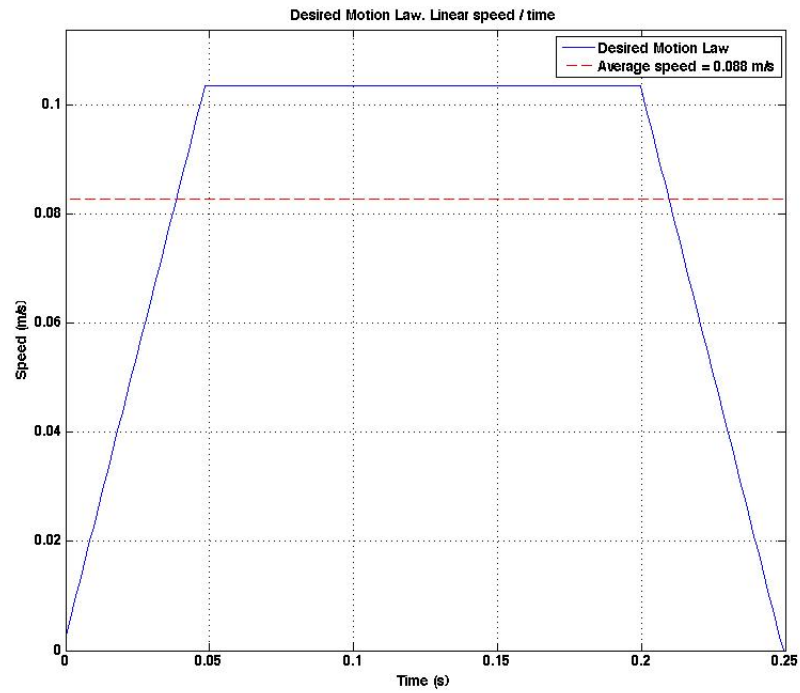


Figure 4: Desired law of motion and average speed

This speed is necessary for the correct electric drive choice and it will be analysed with the transmission system.

2.2.2 Torque requirements

Since there are not technical information about the engine clutch system, the torque calculation is one of the most critic aspects of the problem. It is known from theory that the torque required to the electric drive is composed by multiple terms: one inertial term, due to mass acceleration and deceleration, a term related to friction forces and a term related to springs which gives a term of force which can

be modeled like a single spring working with the Hooke Law. Assuming that the transmission system used is composed by a ball screw or by a gear-head, the following equation can be written:

$$\tau = \frac{F_L r_{eq}}{\eta} \quad (9)$$

Where:

- τ = It is the torque required to the motor.
- F_L = It is the load force, i.e. the sum of spring forces and friction forces.
- r_{eq} = It is the equivalent radius which behaves like a gear ratio for the motor.
- η = It is the transmission efficiency.

As a consequence, considering every part which moves in the system, the equation 9 will have a structure like the following:

$$\tau = \frac{r_{eq}}{\eta} \left(\frac{dv}{dt} M_{tot} + F_a + F_{Hooke} \right) \quad (10)$$

Although equation 10 is apparently simple, it presents some important problems in the calculations. In particular, the difficulties quoted are here analysed:

- The total mass M_{tot} depends on the system position because, when the clutch is not actuated, its discs are connected with each other while transmitting motion from the engine crankshaft to the primary gear shaft. On the other hand, while in unload position, the engine clutch lever is only linked to the discs, not transmitting motion.
- During rotation, discs need to be separated and, when the pulling phase starts, discs load doesn't change linearly, but in a casual way.
- The system has 5 springs to hold the disks in the correct position and, since the clutch system is covered by company secrets, springs must be inserted in the position described by the assembly manual. This leads to disks compressed in an unknown way. In addition, since the engine is closed, it is impossible to calculate the elastic constant and so the required force.
- The friction term of the equation F_a is quite difficult to estimate since it depends on shafts frictions, thermal energy dispersion with oil and various frictions through engine components.

Since the high number of assumptions required for a theoretic approach to the calculation of the maximum torque, it was preferred to measure the forces applied with practical experiments in order to extract the maximum torque required to the electric motor.

2.3 TORQUE REQUIREMENTS EXPERIMENTS

In order to calculate the torque it has been isolated, from now on, the mechanical system of the clutch from the electric motor assuming to connect the two systems with a steel cable. In this way it is possible to separately analyse the two systems and extracting the force on the cable with an experiment and then take back its effect to the motor. By doing this, the calculations for the size estimation can be done with better data. In addition this method allows a better design of the transmission system.

Therefore, two experiments were done to acquire the necessary pulling force.

2.3.1 Hang masses

The first experiment was done in the building where the Race UP Team works, i.e. the OZ Racing factory. The first attempt to analyse the force required was made hanging some weight to a steel cable which was, in turn, connected to the engine clutch lever. Subsequently, by weighing the masses, the first raw estimate of the force could be calculated. (fig. 5, 6)



Figure 5: Masses hanged to the engine clutch lever



Figure 6: Total weight

From this experiment, the force required for the total pulling of the clutch resulted to be:

$$F = mg = 23.3 \cdot 9.81 = 228,6 \text{ N} \quad (11)$$

However, since the experiment took place slowly, it could not be considered a dynamic experiment and so the force obtained could not be considered to contain inertial effects. In fact, considering this result would have led to size the electric drive incorrectly. On the other hand the 228,6 N found can be related, with a certain uncertainty, to the

sum of F_a and F_{Hooke} terms. Still, the experiment result gave some important data about the order of magnitude of the forces.

2.3.2 Structure with torque wrench

Since the first experiment did not give the desired results, a second one had to be made in order to solve the problem of the maximum torque estimation. Therefore, it was necessary to realize a structure attached to the IC engine that would allow, through a torque wrench, the force to be extracted in a very simple and fast way. The schematic design realized is shown in Figure 7.

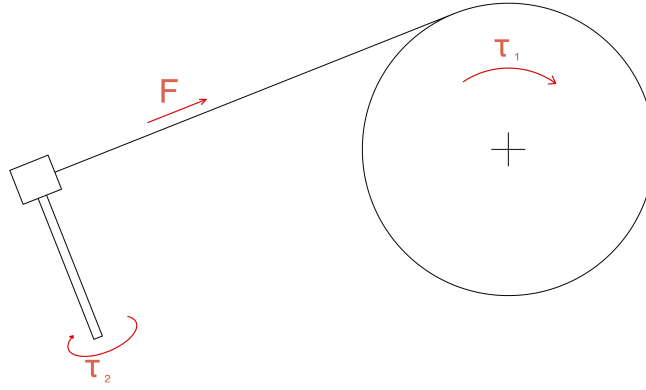


Figure 7: Structure scheme for the maximum force calculation

This experiment allows the user to apply a given torque τ_1 to an aluminium cylinder which, consequently, applies a force applied (F) on the steel cable. As a result, because of the torque wrench working principle, it was possible to set a specific torque and trying to pull the wrench in a specific time; if the torque setting was too low, the torque wrench would have interrupted the torque transmission, with a sound. This allowed a rough evaluation of how the force required changes depending on the speed of actuation. By lowering the times of actuation it was noted that the torque required increased and, when the speed requirements were fulfilled, the resulting torque applied was of 13,5 N m. Therefore, by computing equation 12 it was found out that the required force applied on the cable is 270 N provided that the speed was constant.

$$F = \frac{\tau_1}{R_1} = \frac{13,5 \text{ N m}}{0,05 \text{ m}} = 270 \text{ N} \quad (12)$$

As a result, the torque to apply to the vertical shaft of the clutch can be easily calculated with the following equation:

$$\tau_2 = F \cdot R_2 = 270 \text{ N} \cdot 37 \text{ mm} = 9,99 \text{ N m} \quad (13)$$

These values of force and torque, since executed with speeds compatible with speed requirements, include both static terms F_a and F_{Hooke} of equation 10, but also the dynamic term $\frac{dv}{dt} M_{\text{tot}}$. Experiments just described were made in the laboratory of the University of Padova - Department of Management and Engineering and they are represented in figures 10 and 9.

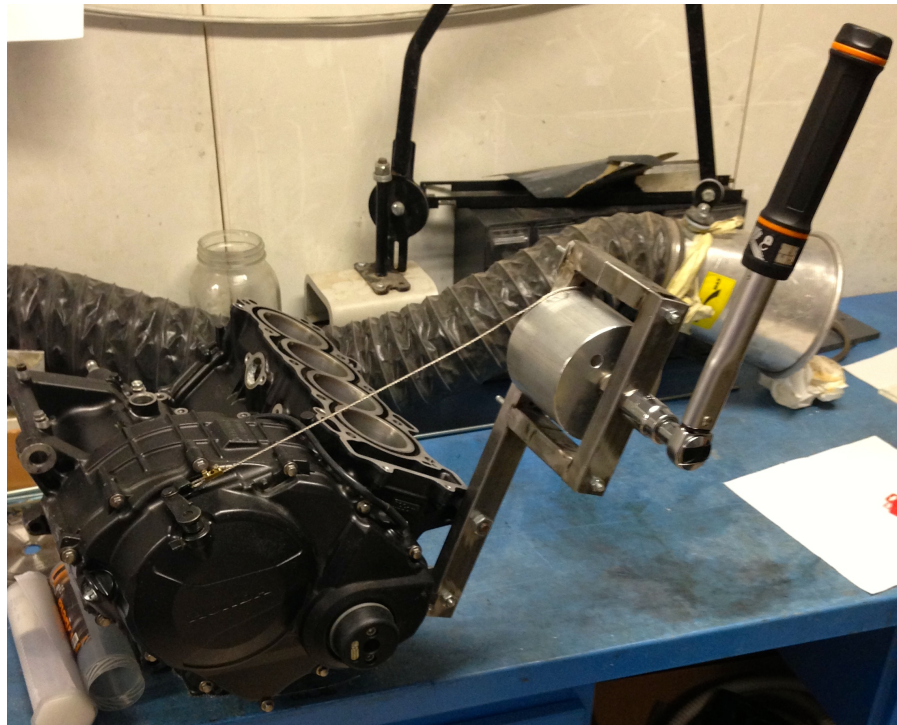


Figure 8: Structure for the force calculation

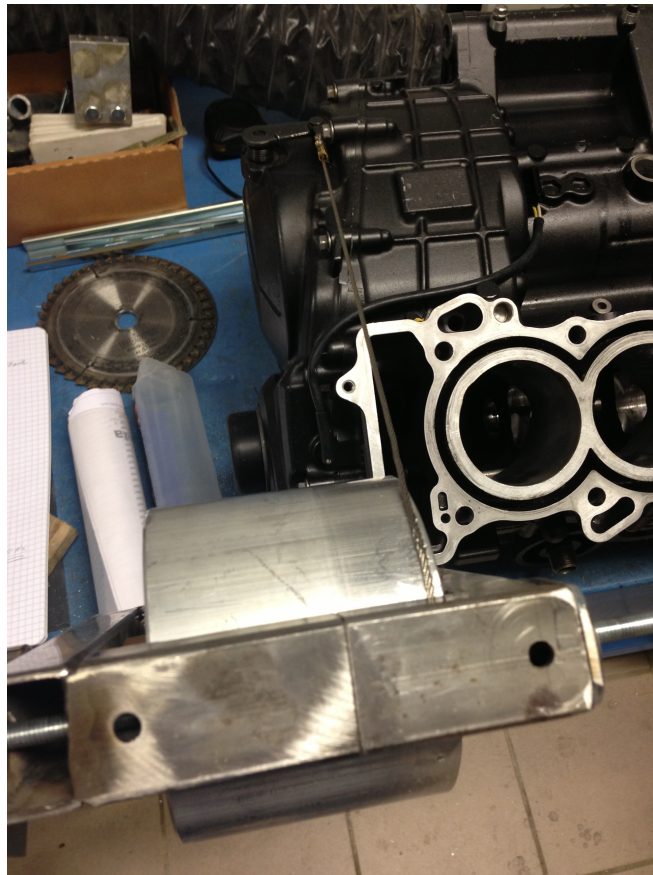


Figure 9: Structure for the force calculation

2.4 TRANSMISSION SYSTEM

After deducing torque and speed requirements it is necessary, for the sizing of the electric motor, to choose a correct motion transmission system. Some solutions were evaluated and they are now presented.

2.4.1 *Motor connected axially to the clutch vertical shaft*

The easiest and simplest solution would be to directly join the actuator rotor directly on the clutch vertical shaft. This solution would allow to reduce the overall inertial effects removing the transmission inertia giving advantages in the motor sizing. Despite that, there are some limitations in the positioning of the electric drive and, in addition, it would be necessary to use gear ratios. This solution can be realized if properly sized and depending on the specific drive.

2.4.2 *Motor with cylinder and cable*

Another possible solution studied is to use a disc axially fixed to the electric motor, with a steel cable rolled up the disc. This way, the

weight problem is solved but there still is the positioning problem since the motor would need to be attached in a precise position and would result projecting outside the chassis of the vehicle. As a result, this option was discarded.

2.4.3 Ball screw

In this preliminary analysis the solution that best fits to the design objectives was to use a transmission system based on a ball screw. This option allows, with a discrete weight, to have a correct positioning of the motor in the space of the vehicle allowed. For these reasons it was chosen to pick one specific set of ball screws and evaluate every solution while sizing the electric actuators. After choosing the best motor a final analysis of the best transmission system could be done, in order to improve the overall final design. As a consequence SKF was chosen to be the case study company, since it is a well consolidated company with a very well documented technical sheets. After downloading the catalogue several right hand leads were considered and, through equations 14 the equivalent radius could be calculated.

$$r_{eq} = \frac{p}{2 \cdot \pi} \quad (14)$$

As observed before, in equation 10, the total torque to require to the motor is given by the sum of a static term and a dynamic one; for this reason, changing the equivalent radius causes the gear ratio between the motor and the engine clutch lever to change which, in turn, changes the maximum torque and the maximum speed required to the motor. As a result, if the peak torque required to the motor lowers, the top speed rises which makes the inertial term to rise. From the calculations it emerged that it exists a function that presents a minimum in power that the actuator has to supply in order to complete the task. It was found out that completely locking the transmission system would make the motor choice too limited making the comparison between different kind of actuators impossible. For these reasons, it was decided to use the SKF ball screws for motors sizing, choosing between models SN/BN/PN or SL/BL ones, and define the exact right hand lead of the ball screw in every actuator section. In conclusion, the data used in the motors sizing was:

- Peak force on the steel cable = $F = 270 \text{ N}$
- Top linear speed of the steel cable = $\text{Speed}_{peak} = 0.11 \frac{\text{m}}{\text{s}}$

As said before, the transmission system will be sized with the electric drive. So, from the SKF catalogue ball screw right hand leads of 5, 10, 20, 25, 32, 40 or 50 mm were chosen to be considered during the calculations.

Nuts for ball screws

Nuts for ball screws




Screw assembly		Type of recirculation		Right hand lead		Axial play		Backlash elimination		Preload for optimum rigidity		Nut accessories		Screw accessories		Catalogue page		
				Diameter														
SD/BD		Internal, by inserts		8	2,5	SD	BD									14		
				10	2 - 4	SD	BD											
				12	2 - 4 - 5	SD	BD											
				14	4	SD	BD											
				16	2 - 5 - 10	SD	BD					yes						
SDS/BDS		Stainless steel optional														16		
SH		External, by integrated tube		6	2	SH										18		
				10	3	SH												
				12,7	12,7	SH												
SHS		Stainless steel optional														16		
SX/BX		Internal, by inserts		20	5	SX	BX			yes	yes					20		
				25	5 - 10	SX	BX			yes	yes							
				32	5 - 10	SX	BX			yes	yes							
				40	5 - 10	SX	BX			yes	yes							
				50	10	SX	BX			yes	yes							
				63	10	SX	BX			yes	yes							
SND/BND/PND		Internal, by inserts		16	5 - 10	SND	BND	PND				yes				24		
				20	5	SND	BND	PND				yes						
				25	5 - 10	SND	BND	PND				yes						
				32	5 - 10	SND	BND	PND				yes						
				40	5 - 10	SND	BND	PND				yes						
				50	10	SND	BND	PND				yes						
				63	10	SND	BND	PND				yes						
DIN VERSION																		
SN/BN/PN		Internal, by inserts		16	5	SN	BN	PN				yes				28		
				20	5	SN	BN	PN				yes						
				25	5 - 10	SN	BN	PN				yes						
				32	5 - 10	SN	BN	PN				yes						
				40	5 - 10	SN	BN	PN				yes						
				50	10	SN	BN	PN				yes						
				63	10	SN	BN	PN				yes						
SL/BL - SLD/BLD		By faces		25	20 - 25	SL	BL					yes				32		
				32	20 - 40	SL	BL					yes						
				32	32	SL	BL					yes						
				32	32	SLD	BLD					yes						
				40	20 - 40	SL	BL					yes						
				50	50	SL	BL					yes						
SLT, BLT, Rotating nuts										with SL/BL long lead screw					34			
Accessories: FLBU, PLBU, BUF																40		

Figure 10: SKF Catalogue

STEPPER MOTOR SIZING

As said before, the aim of this script is to size an electric drive to perform a complete motion of the clutch lever. In this chapter a stepper motor is chosen as first attempt to complete the said task. First of all, general information about the structure of the motor will be given, then the reader will find the analysis of the requirements depending on the motor chosen.

3.1 STEPPER MOTORS - INTRODUCTION

Stepper motors main feature is that the rotation is made through a sequence of regular steps of a given angle. The principle of operation is based on magnetic flux. *“Magnetic flux crosses the small airgap between teeth on the two parts of the motor. According to the type of motor, the source of flux may be a permanent-magnet or a current-carrying winding or a combination of the two. However, the effect is the same: the teeth experience equal and opposite forces, which attempt to pull them together and minimise the airgap between them.”* [2].

If compared to other kind of motors, these ones present some advantages:

- They can assume precise positions without using position or speed sensors.
- The positioning error does not add up in multiple positioning.
- They are fairly simple to be digitally controlled.

Depending on their structure, the operating principle can be based on different magnetic flux sources and, by sorting motors depending on that aspect, three categories can be selected:

- Switched reluctance motors.
- Permanent magnet step motors.
- Hybrid step motors.

3.1.1 Switched reluctance motors

“In the variable-reluctance stepping motor the source of magnetic flux is current- carrying windings placed on the stator teeth. These windings are excited in sequence to encourage alignment of successive sets of stator and rotor teeth, giving the motor its characteristic stepping action.” [2]

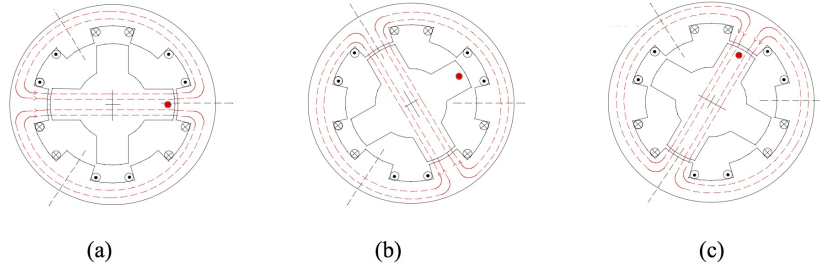


Figure 11: Switched reluctance motor operating principle [4]

These motors have a structure as represented in Fig. 11 and they are usually built with more than one level and, for this reason, they are called “multi-stack”. “The multi-stack variable-reluctance stepping motor is divided along its axial length into magnetically isolated sections (‘stacks’), each of which can be excited by a separate winding (‘phase’).” [2] This solution allows the switched reluctance motors to have better resolution and precision.

3.1.2 Permanent magnet motors

In this kind of stepping motors the rotor is built with a cylindrical permanent magnet which creates a permanent magnet field and flux. The windings of the different phases are sequentially excited by current which creates a magnetic field which, as a result, produces the torque pulling the magnet. By continuously switching the excited phase, the motor rotates with a sequence of steps. The section of the motor is represented in Fig. 12.

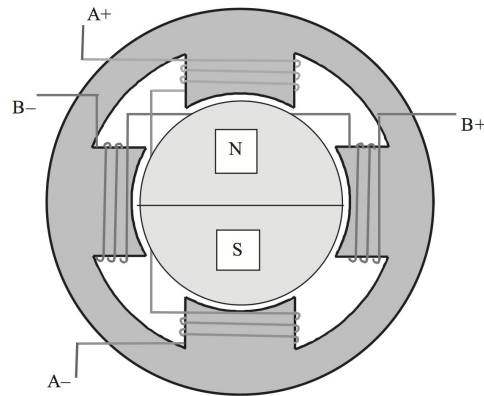


Figure 12: Permanent magnet motors [2]

These motors are more convenient for some aspects here presented:

- High detent torque.
- Fast positioning.

3.1.3 Hybrid stepping motors

“The hybrid stepping motor has a doubly salient structure, but the magnetic circuit is excited by a combination of windings and permanent magnet. Windings are placed on poles on the stator and a permanent magnet is mounted on the rotor. [...] The stator poles are also provided with windings, which are used to encourage or discourage the flow of magnet flux through certain poles according to the rotor position required. “[2] By repeatedly switching phases, the rotary motion is created as a succession of steps.

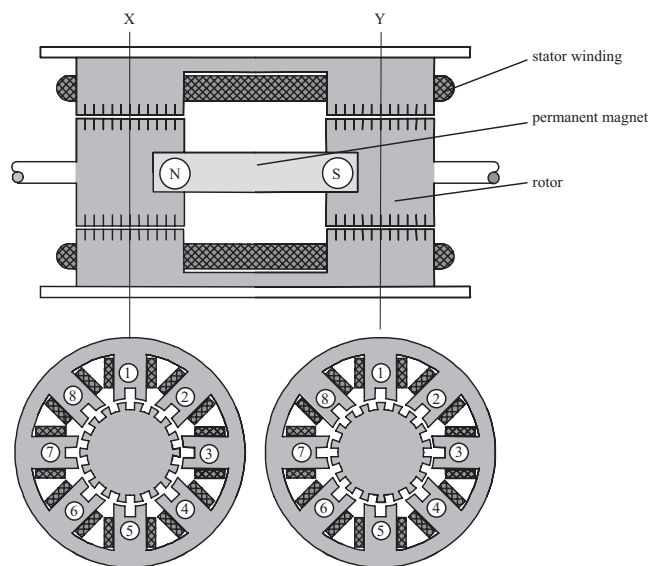


Figure 13: Side view and cross-sections of a hybrid stepping motor [2]

These kind of motors have some advantages if compared to the previous kinds:

- Speed: it is faster than both switched reluctance motors and the permanent magnet ones.
- Pullout torque curve: it is the dynamic torque characteristic and it is better than the other ones.
- Efficiency.
- Resolution: for the hybrid motors there usually are smaller step angles and, as a consequence, more steps per revolution.
- Precision: better resolution leads to better precision.

On the other hand hybrid motors are more expensive because they are more difficult to produce and they require smaller construction tolerances.

3.2 STEPPER MOTOR SIZING

In this section the stepper motor sizing will be analysed in different steps using the speed and torque requirements calculated and summed up in paragraph 2.4.3. Then, by browsing different companies catalogs, different motors were compared to the requirements and the results will be presented showing the dependencies between the power required to the motor and the right hand lead of the ball screw. After that, a comparison between the motor pullout torque and the various motor required powers depending on the right hand lead will be done. Finally, when the comparisons are complete, the safety factor, the weight and the cost of the motors will be considered, and then the final choice will be made. For the final choice, a MATLAB® simulation will be done in order to calculate every parameter in every moment of the motion of the motor.

Given that some parameters are common to every motor and need to be part of the calculations, they can be considered as follows:

- Right hand lead: as seen in section 2.4.3.
- Equivalent radius: as seen in equation 14.
- Screw Inertia, as given in the product datasheet.
- Motor speeds: calculated with the following equation.

$$\omega = \frac{Speed_{peak}}{R_{eq}} \left[\frac{rad}{s} \right] \quad (15)$$

and then converted to different measuring units in order to compare them with the ones given in different datasheets.

- Static Torque: it is the torque needed to complete the motion in an infinite amount of time. It is calculated with equation 16.

$$\tau_{static} = \frac{F \cdot Speed_{peak}}{\omega \cdot \eta} [Nm] \quad (16)$$

- Static Power: it is the power required to complete the motion in an infinite amount of time. It is calculated with equation 17.

$$P_{static} = \tau \cdot \omega [W] \quad (17)$$

These calculation are here presented in Fig. 14 for each Right hand lead.

In the following subsections inertial torques will be calculated (eq. 18)and added to the static torques and, after that, the total power required to the motor will be considered to find the best right hand lead for the specific motor.

$$\tau_{dynamic} = (I_{screw} + I_{motor}) \cdot \left(\frac{d\omega}{dt} \right) [Nm] \quad (18)$$

Right Hand Lead[m]	Req [m]	Screw Inertia[kg m ²]	Motor Speed [rad/s]	Motor Speed [rpm]	Motor Speed [rps]	Motor Speed [pps]	Static Torque [Nm]	Static Power [W]
0.005	0.0008	3.30E-05	138	1320	22	4400	0.25	34.9
0.010	0.0016	2.15E-04	69	660	11	2200	0.51	34.9
0.020	0.0032	2.15E-04	35	330	6	1100	1.01	34.9
0.0300	0.0048	2.10E-04	23	220	4	733	1.52	34.9
0.040	0.0064	6.00E-04	17	165	3	550	2.02	34.9
0.050	0.0080	1.33E-03	14	132	2	440	2.53	34.9

Figure 14: Static calculations with ball screw

$$\tau_{\text{total}} = \tau_{\text{dynamic}} + \tau_{\text{static}} [\text{N m}] \quad (19)$$

$$P_{\text{total}} = \tau_{\text{total}} \cdot \omega [\text{W}] \quad (20)$$

In addition, for some motors, a safety factor was calculated. Given that torque estimations were made through a mechanical system, a safety factor of 50% is considered to be a requirement for the motor sizing. This condition is based on uncertainties of the project which could be fulfilled by testing different motors and analysing the parameters during the motion. Anyway, these tests require to buy multiple motors, which is an unacceptable solution because of the limited budget available. Moreover, since the spirit of the competition is to build a reliable car, guaranteeing the motion in every condition is the first priority.

3.2.1 Anaheim Automation 34K314S-LW8

In this section, the motor 34K314S-LW8 from Anaheim Automation will be analysed. It is a NEMA 34 size stepper motor which weighs 5.4 kg.

As it can be observed in Fig. 15 and 16 the power required to the motor has a minimum, which is represented in row 5.

In Fig. 17 it can be observed a comparison between the required total torques and the pullout torques required by the motor. Given a specific ball screw, its right hand lead sets a working point in terms of speed and torque required to the motor. By calculating all these working points a curve is created which can be compared to the pull-out torque. This motor well fits the requirements for low speeds but it does not for high speeds so, it requires ball screws with longer right hand leads. Since the operating principle of steppers motors is that their rotation is composed by multiple steps it is technologically complex to reach high speeds and, as a result, this result could be expected.

Inertial Torque [Nm]	Total Torque [Nm]	Total Torque [Oz in]	Total Power [W]
1.20	1.46	206	201.4
0.85	1.36	192	93.9
0.43	1.44	204	49.7
0.28	1.80	255	41.4
0.35	2.37	335	40.9
0.48	3.01	426	41.6

Figure 15: Anaheim Automation 34K314S-LW8 total power calculations

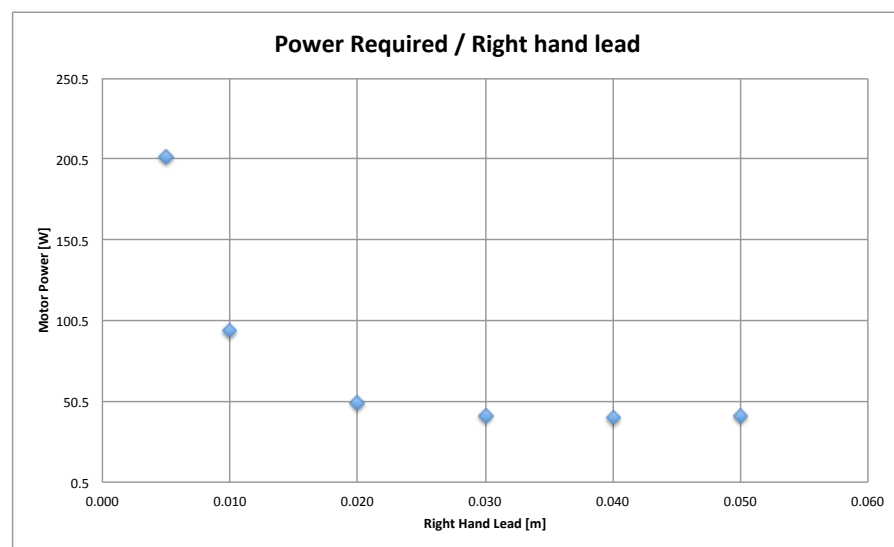


Figure 16: Anaheim Automation 34K314S-LW8 torque required vs right hand lead

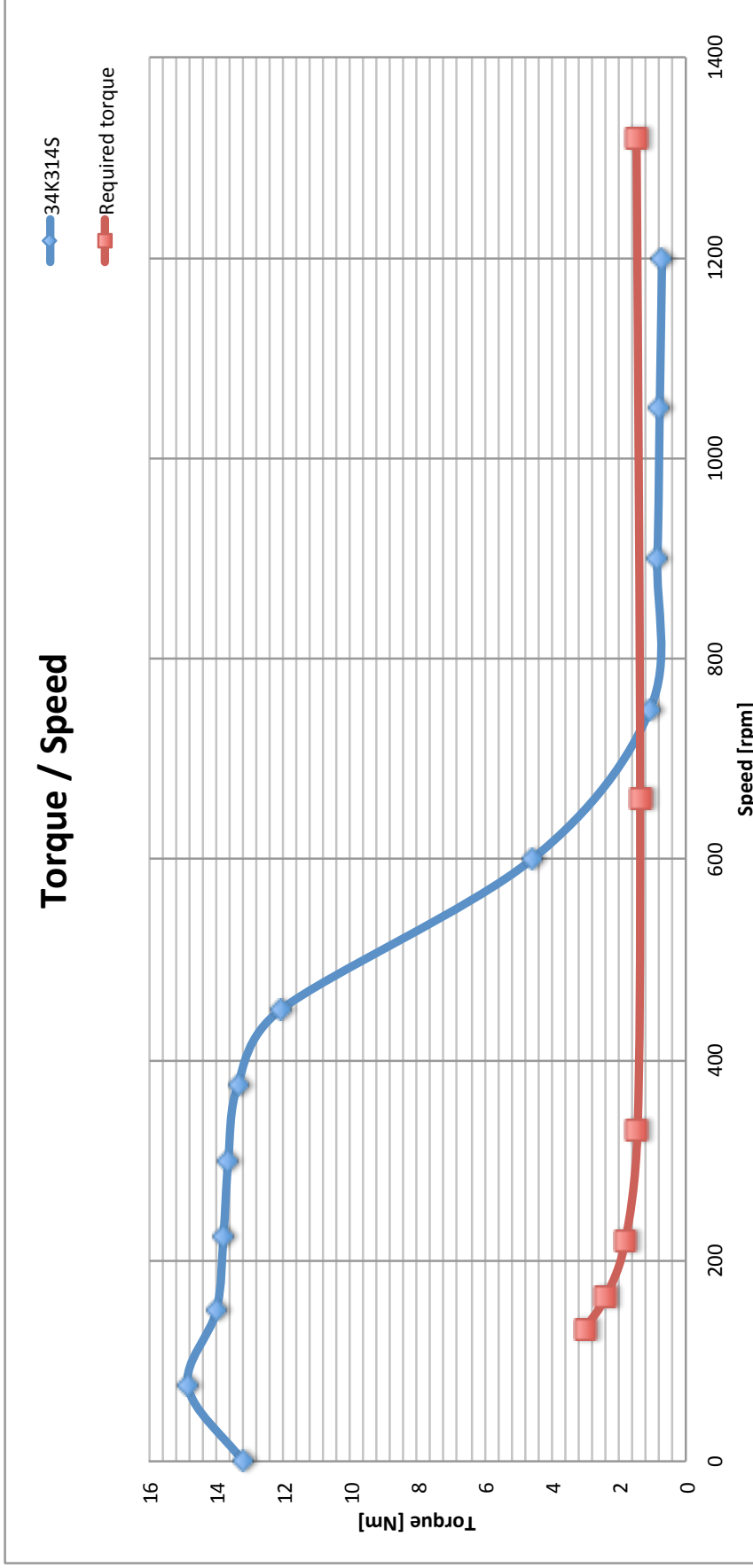


Figure 17: Anaheim Automation 34K314S-LW8 and required power comparison

3.2.2 *Anaheim Automation 34K112S-LW8*

In this section, the motor 34K112S-LW8 from Anaheim Automation will be analysed. It is a NEMA 34 size stepper motor which weighs 2.26 kg.

As it can be observed in Fig. 18 and 19 the power required to the motor has a minimum, which is represented in row 4. This power value is lower than the previous value because the inertia of Anaheim Automation 34K112S-LW8 is lower than the 34K314S-LW8 model. As the previous model and as it can be observed in Fig. 20, this motor well fits the requirements for every speed. In this case, in fact, having the motor a lower rotor inertia, it is able to keep higher speeds without losing steps.

Nevertheless, these NEMA 34 motors, i.e. the Anaheim Automation 34K314S-LW8 and the Anaheim Automation 34K112S-LW8 cannot be chosen for the application: by browsing the website it is said that these pullout curves are given with specific drivers of the same company and that NEMA 34 stepper motors drivers require a supply voltage of 120 VAC. As said in the beginning, the supply voltage available on the vehicle is a battery which can supply up to 14 VDC. As a result, smaller motors must be considered.

Inertial Torque [Nm]	Total Torque [Nm]	Total Torque [Oz in]	Total Power [W]
0.48	0.73	104	101.5
0.49	1.00	141	69.0
0.25	1.26	178	43.4
0.16	1.68	238	38.7
0.26	2.28	323	39.4
0.41	2.93	416	40.6

Figure 18: Anaheim Automation 34K112S-LW8 total power calculations

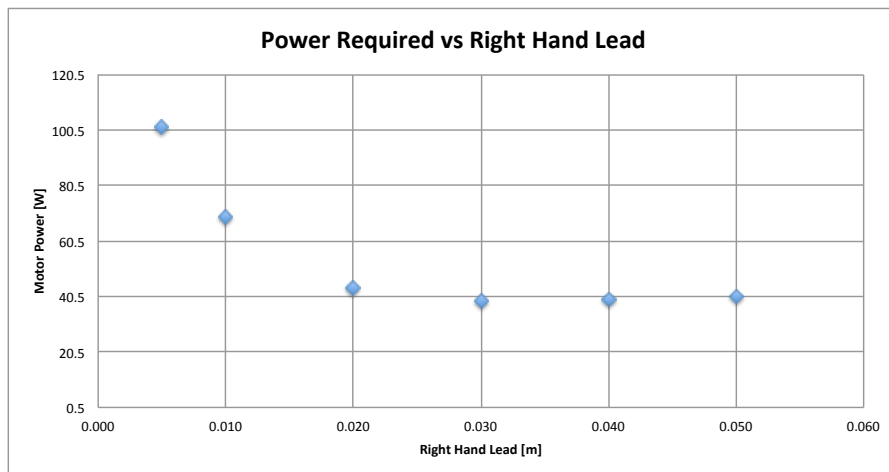


Figure 19: Anaheim Automation 34K112S-LW8 torque required vs right hand lead

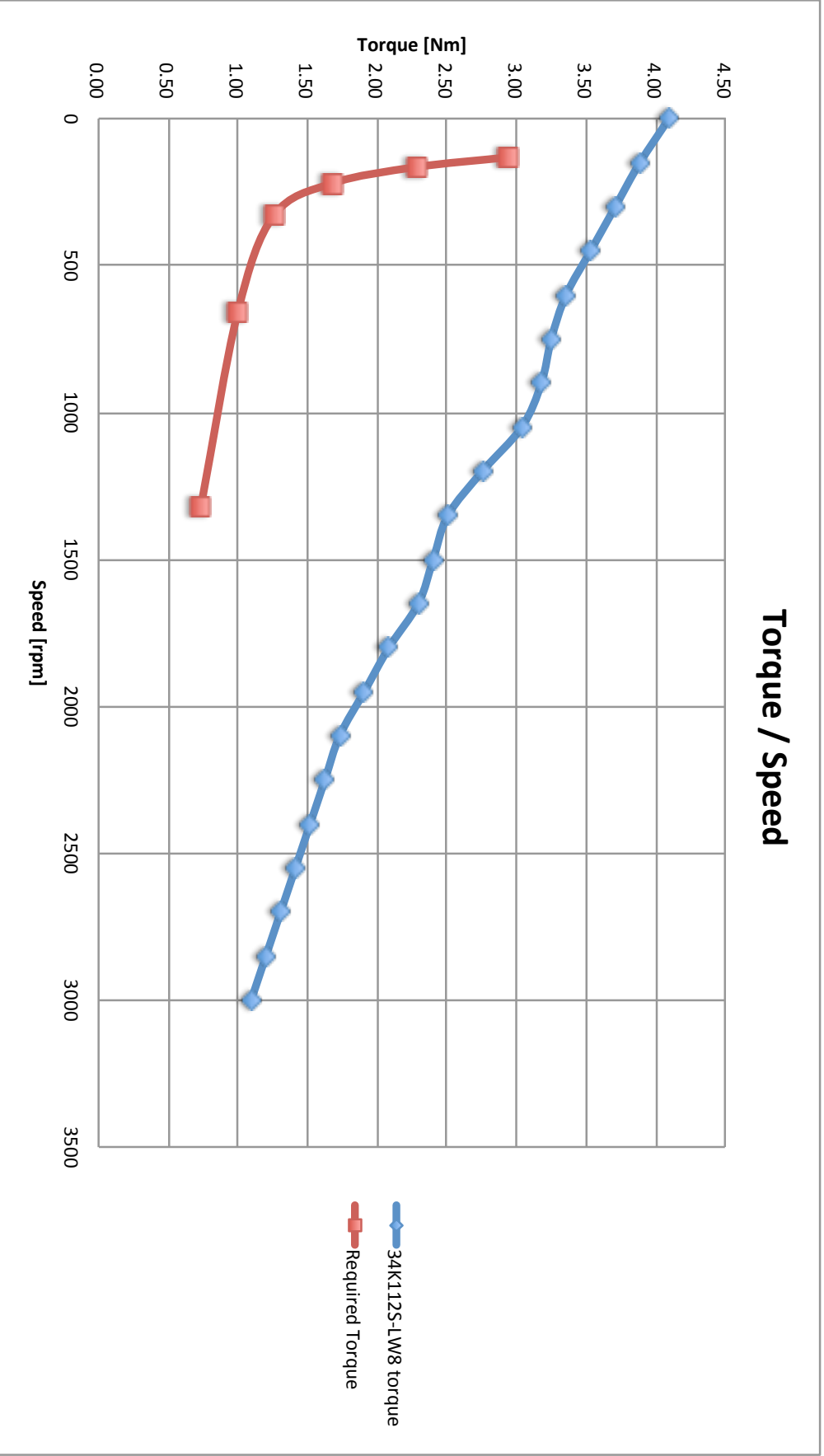


Figure 20: Anaheim Automation 34K112S-LW8 and required power comparison

3.2.3 Anaheim Automation 24Y504S-LW8

In this section, the motor 24Y504S-LW8 from Anaheim Automation will be analysed. It is a NEMA 24 size stepper motor which weighs 1.4 kg.

As it can be observed in Fig. 21 and 22 the power required to the motor has a minimum, which is represented in row 4. As it can be observed in Fig. 23, this motor does not fit the requirements because of its too low pullout curve. The two best points are the ones represented in rows 3 and 4 of Fig. 21 which corresponds to 330 rpm and 220 rpm respectively. Given that at 220 rpm the pullout torque is about 1.75 Nm and at 220 rpm the required torque is 1.65 Nm the safety factor is:

$$\nu_1 \cong 6\% \quad (21)$$

This motor could have solved the supply voltage problems of the previous models because it requires a 24 VDC supply which can be achieved with a boost converter which can amplify the input voltage. This allows to have 24 VDC from the only 14 VDC available. Nevertheless, this motor cannot be considered valid for the application because, being the torque curves given as drawings in Torque [oz-in] vs [rps], care must be taken and it must be considered possible truncations while converting measurement units. Also, having extrapolated the speed and torque requirements with experiments, some errors might have been committed so a safety factor of 6% is too low to correctly pick the motor.

Inertial Torque [Nm]	Total Torque [Nm]	Total Torque [Oz in]	Total Power [W]
0.32	0.58	82	79.7
0.41	0.92	130	63.5
0.21	1.22	172	42.1
0.14	1.65	234	38.1
0.24	2.26	320	39.0
0.39	2.92	413	40.3

Figure 21: Anaheim Automation 24Y504S-LW8 total power calculations

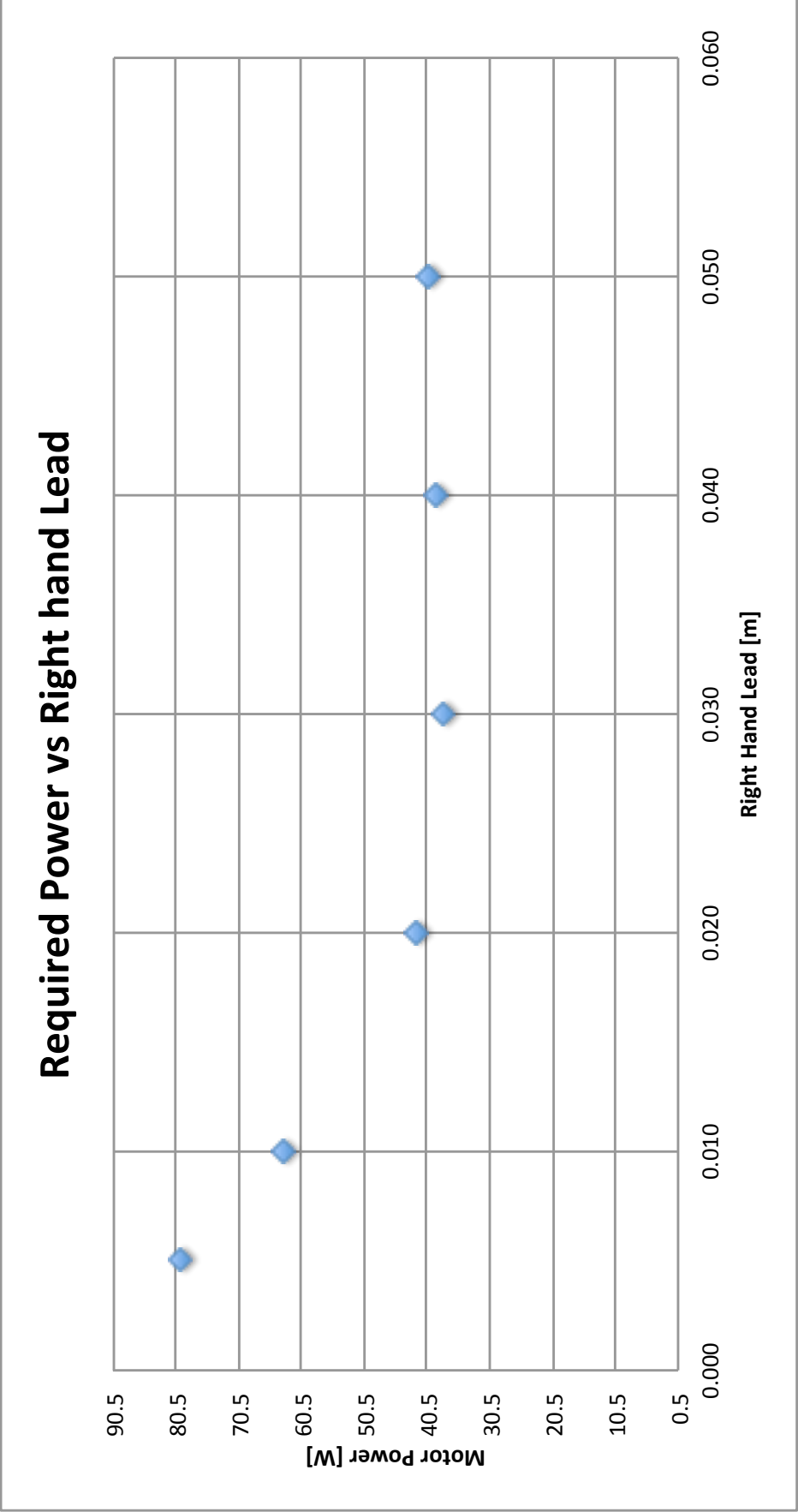


Figure 22: Anaheim Automation 24Y504S-LW8 torque required vs right hand lead

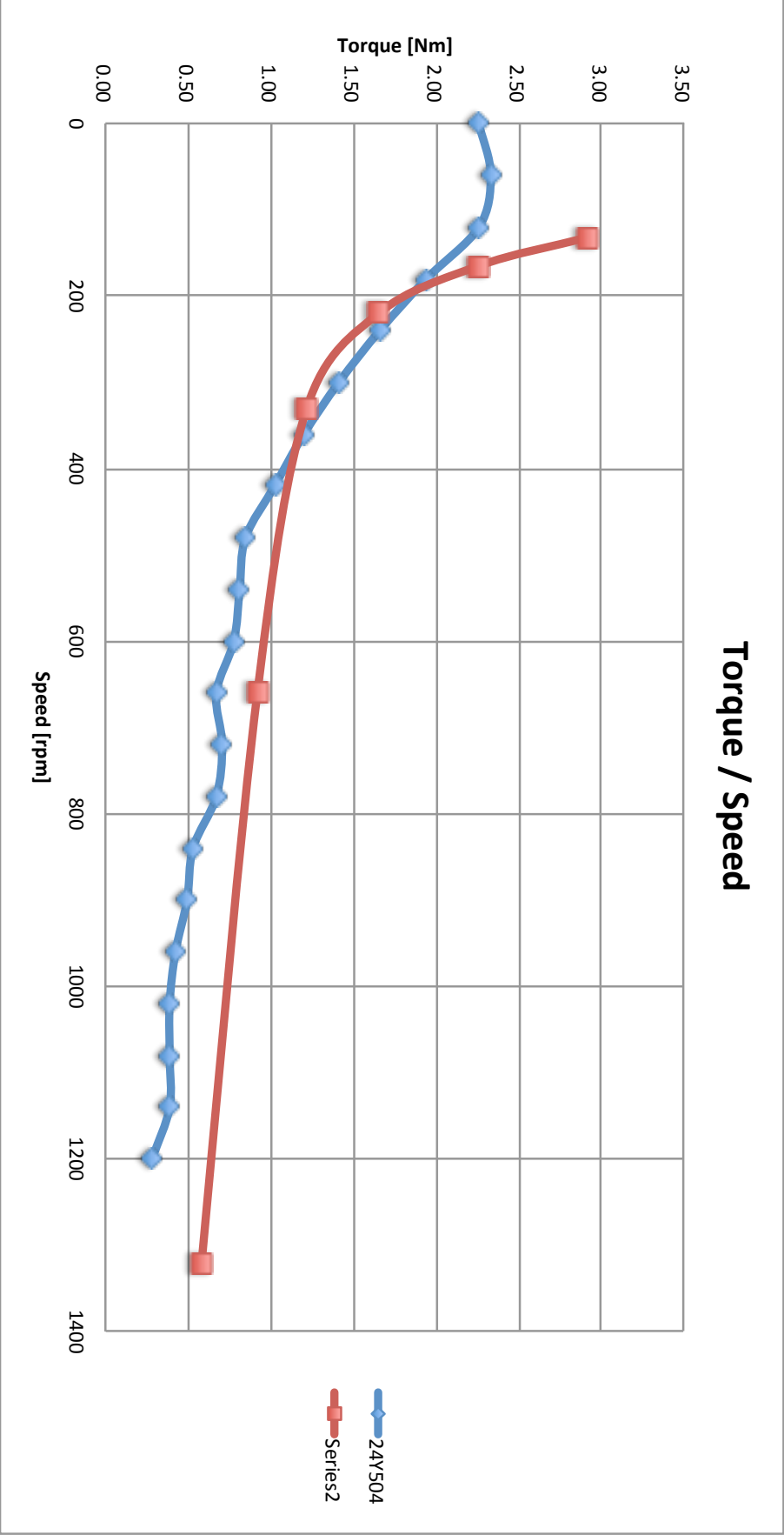


Figure 23: Anaheim Automation 24Y504S-LW8 and required power comparison

3.2.4 Anaheim Automation 24Y508S-LW8

In this section, the motor 24Y508S-LW8 from Anaheim Automation will be analysed. It is a NEMA 24 size stepper motor which weighs 1.4 kg. It is the same size and weight of the previous model but it differs for the pullout torque curve.

As it can be observed in Fig. 24 and 25 the power required to the motor has a minimum, which is represented in row 4 as before. As it can be observed in Fig. 26, this motor is better than the previous one but it still does not quite fit the requirements.

The best point is the one represented in row 4 of Fig. 24 which corresponds to 220 rpm. Given that at 220 rpm the pullout torque is about 2.02 Nm and at 220 rpm the required torque is 1.65 Nm the safety factor is:

$$v_2 \cong 22\% \quad (22)$$

Inertial Torque [Nm]	Total Torque [Nm]	Total Torque [Oz in]	Total Power [W]
0.32	0.58	82	79.7
0.41	0.92	130	63.5
0.21	1.22	172	42.1
0.14	1.65	234	38.1
0.24	2.26	320	39.0
0.39	2.92	413	40.3

Figure 24: Anaheim Automation 24Y504S-LW8 total power calculations

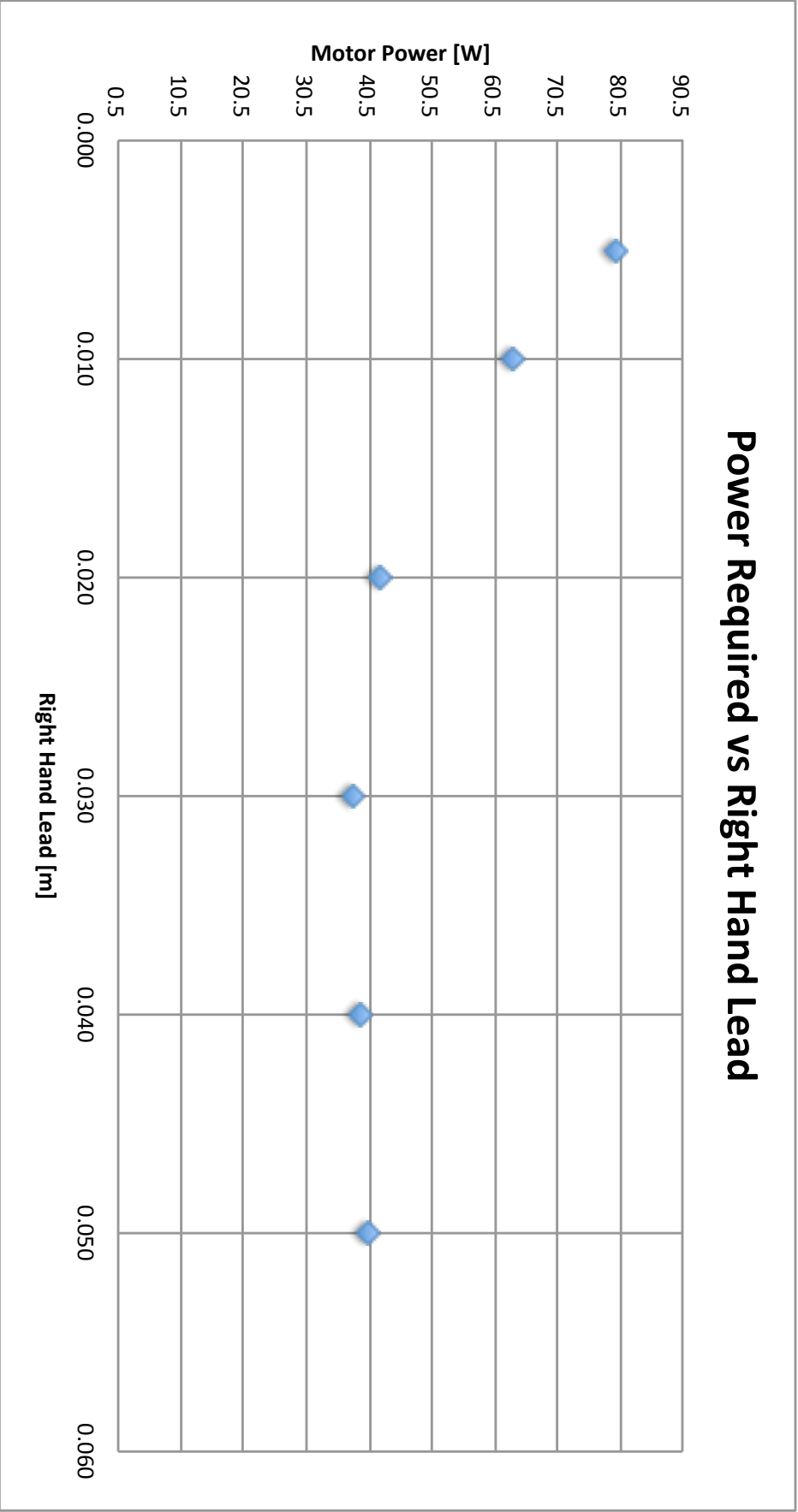


Figure 25: Anaheim Automation 24Y5o4S-LW8 torque required vs right hand lead

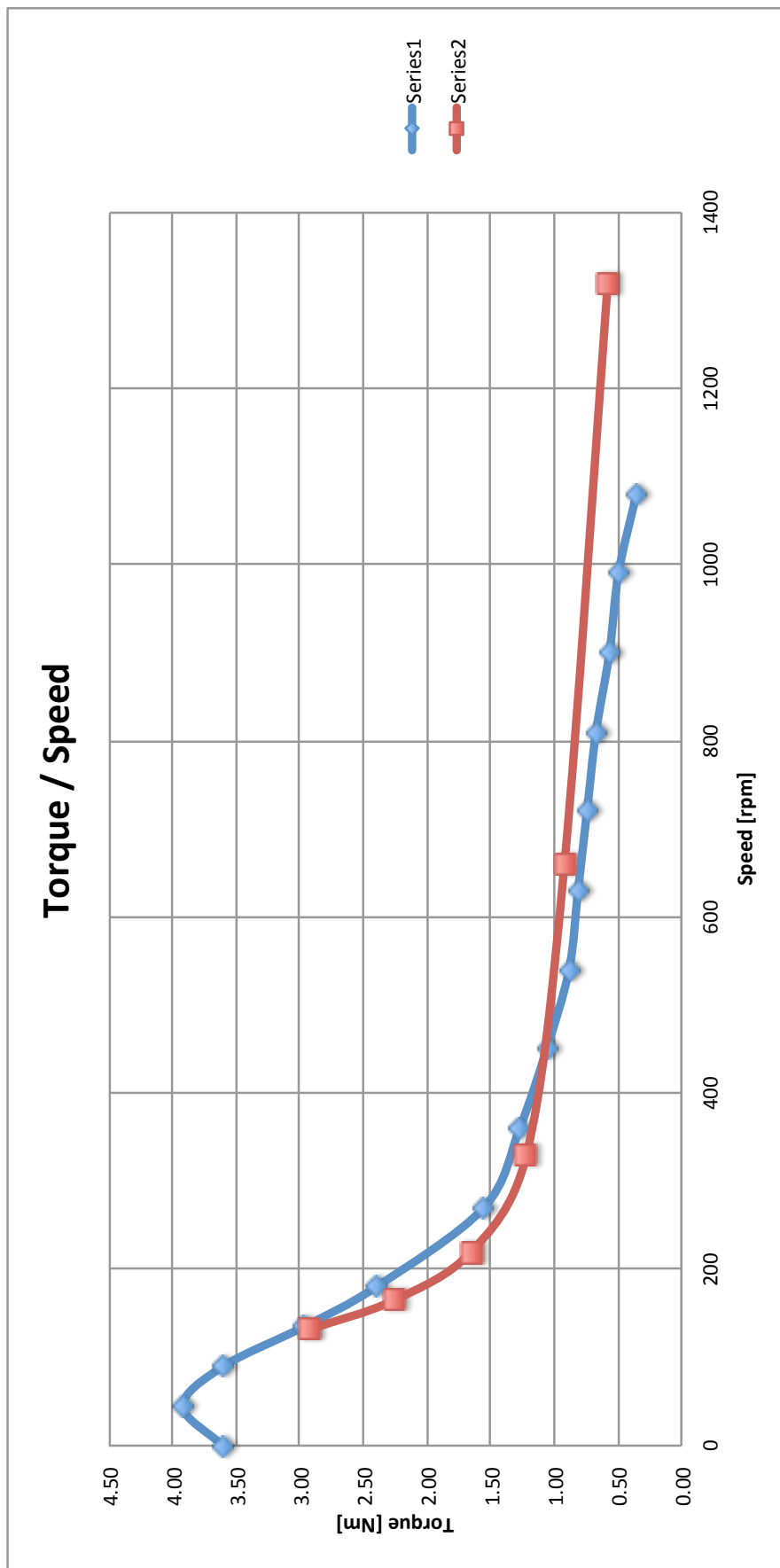


Figure 26: Anaheim Automation 24Y504S-LW8 and required power comparison

3.2.5 Applied Motion HT34-504

Since all the possible motors of Anaheim Automation have been analysed, in this section the motor HT34-504 from Applied Motion will be analysed. It is a NEMA 34 size stepper motor which weighs 1.58 kg.

As it can be observed in Fig. 27 and 28 the power required to the motor has a minimum, which is represented in row 4 as before. As it can be observed in Fig. 29, this motor is quite good for the application. It is supplied with 24 VDC and its weight is acceptable.

The best point is the one represented in row 3 of Fig. 29 which corresponds to 330 rpm. It can be observed that the lowest power one is the one shown in the 4th row. Nevertheless, the best working point is the third one, since it better fits the pullout torque curve. So, after calculating the available torque at 330 rpm, which results 2.335 Nm, the safety factor can be calculated:

$$\nu_3 \cong 88\% \quad (23)$$

As said before, this safety factor is sufficient to cover the 50% required by the project and it is considered sufficient to assure the motion completion.

Coppia Inerziale [Nm]	Coppia Tot [Nm]	Coppia Tot [Oz-in]	Pot Motore [W]
0.40	0.65	92	89.7
0.45	0.96	135	66.0
0.22	1.24	175	42.7
0.15	1.66	236	38.3
0.25	2.27	321	39.2
0.40	2.93	414	40.4

Figure 27: Applied Motion HT304-504 total power calculations

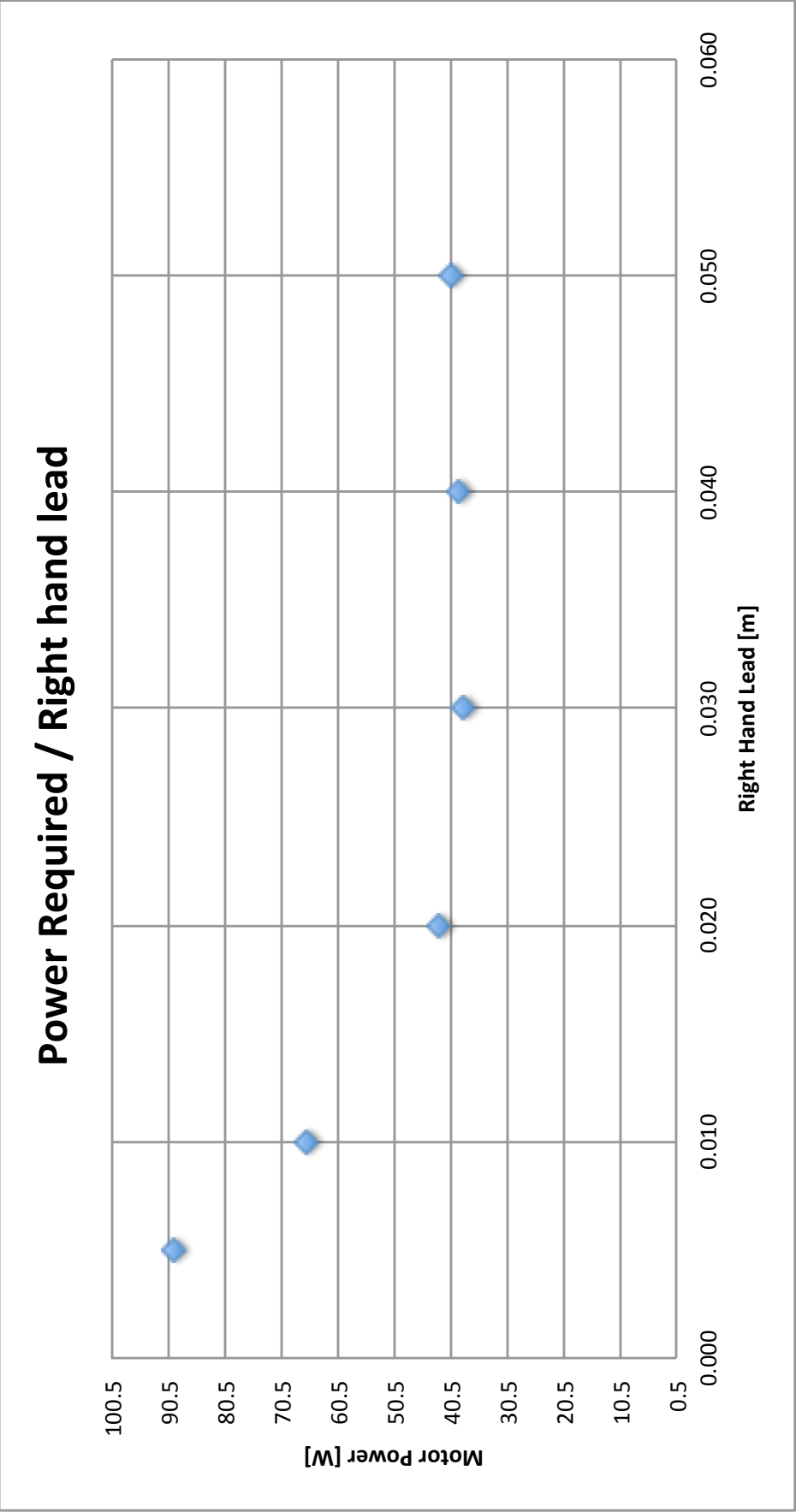


Figure 28: Applied Motion HT304-504 torque required vs right hand lead

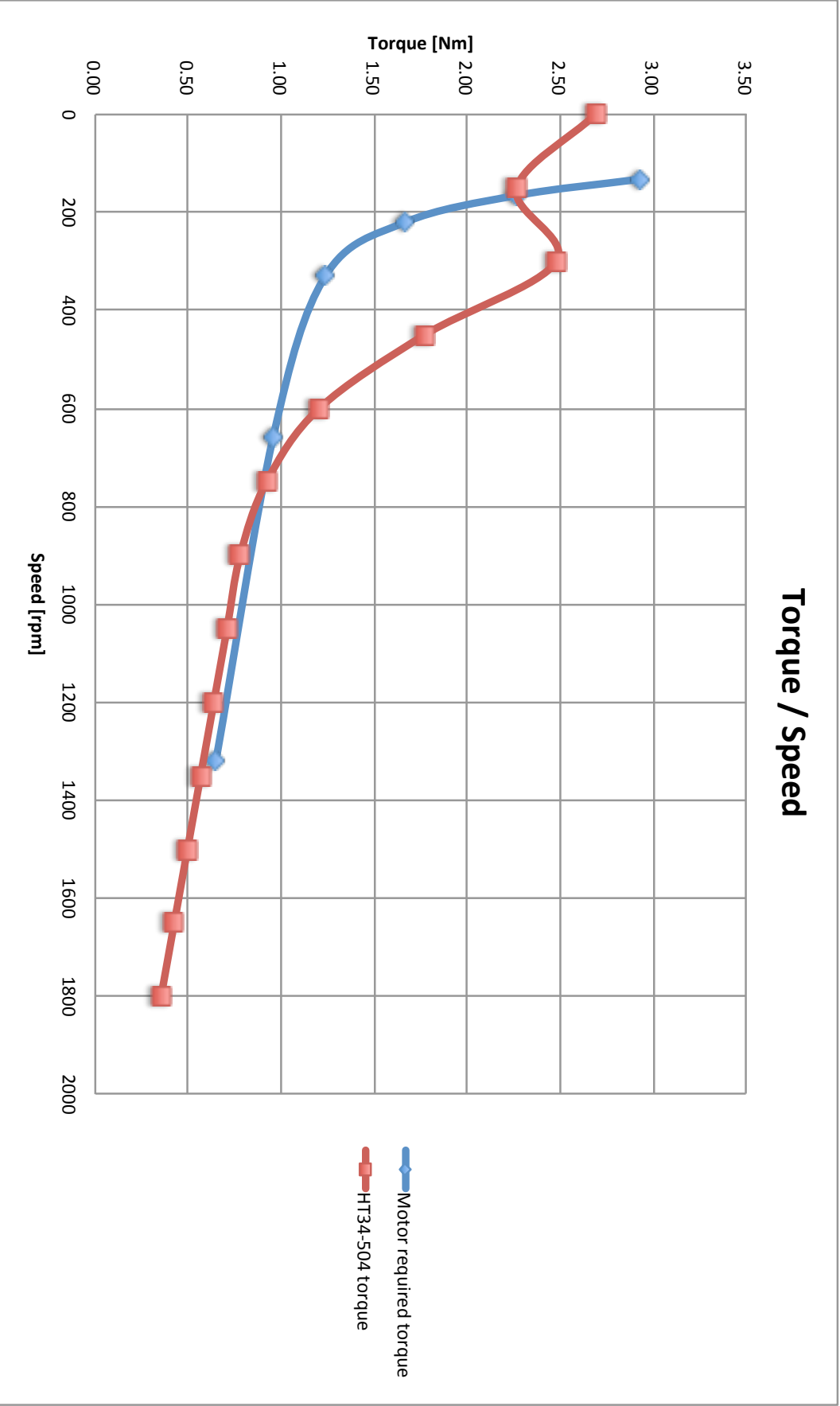


Figure 29: Applied Motion HT304-504 and required power comparison

3.2.6 Comparison

As it can be understood from Fig. 30 the best choice for this application is the HT34-504 motor. It offers a better safety factor and it costs less than the others. The second best choice would be the 24Y508S-LW8 motor which allows a weight reduction but, given the way the initial hypothesis were calculated, there could be some vagueness in the actual loads required and the torque wrench experiment should not be considered precise. Using a load cell could allow to have precise data and to reduce the size of the motor but, not being in these conditions, imposes the choice of the HT34-504 actuator.

Motor	Cost [€]	Weight [kg]	Supply	Safety Factor
34K314S-LW8	\$ 954.00	5.40	120VAC	NA
34K112S-LW8	\$ 479.00	2.26	120VAC	NA
24Y504S-LW8	\$ 139.00	1.40	24 VDC	6%
24Y508S-LW8	\$ 139.00	1.40	24 VDC	22%
HT34-504	\$ 108.00	1.59	24 VDC	88%

Figure 30: Comparison of different motors

3.3 MATLAB® SIMULATION

In order to better understand how the motor chosen operates, a MATLAB® simulation was made. The code is reported in App. A for a better understanding of the process. Here the results are reported. As said before, since the calculations were done for the most critic working point, a simulation was done to monitor various parameters of the motor chosen in every moment of the motion. This way, every working point of the motor was calculated and it was compared to the pullout curve, in order to verify the calculations made. With the said simulation, these plots were produced:

1. Desired speed law of linear speed vs time.
2. Desired speed law of angular speed of the motor vs time.
3. Desired speed law of angular speed of the motor in sps vs time.
4. Torque required to the motor vs time.
5. Torque required to the motor vs speed required.

6. Torque required to the motor compared to the pullout curve of the chosen motor vs speed required.
7. Commutation period vs time.

3.3.1 Linear speed vs time

As said before, the desired speed law is given as hypothesis and it has decided to be as presented in Fig. 31.

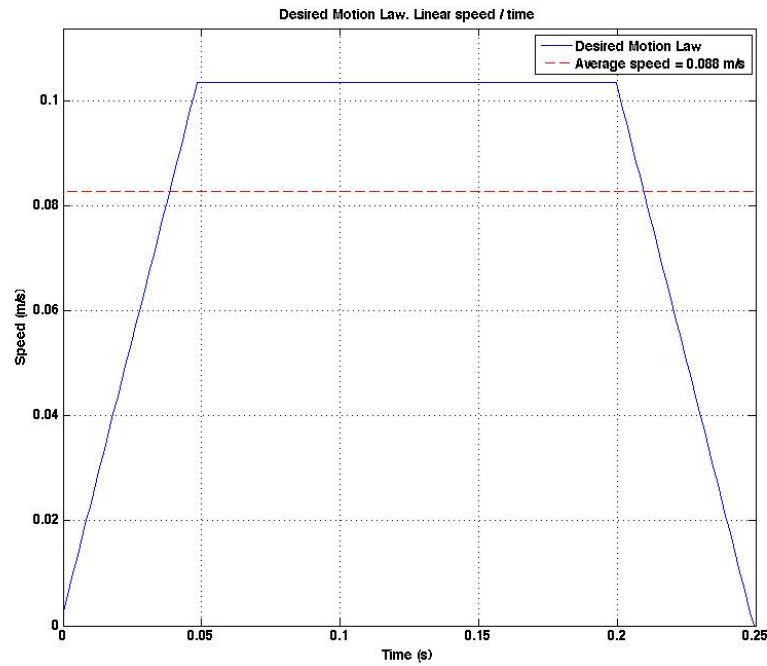


Figure 31: Desired linear law of speed

3.3.2 Angular speed vs time

After that, given that the ball screw right hand lead gives an equivalent radius of 3.2 mm, the linear speed must be linked to an angular speed of the motor. This produces a speed law for the motor which is represented in Fig. 32

3.3.3 Angular speed in pps vs time

In order to calculate the commutations period, it is necessary to calculate the angular speed of the motor expressed in steps per seconds. Of course, the plot will be identical to the previous one but the measurement units will be different. This can be observed in Fig. 33.

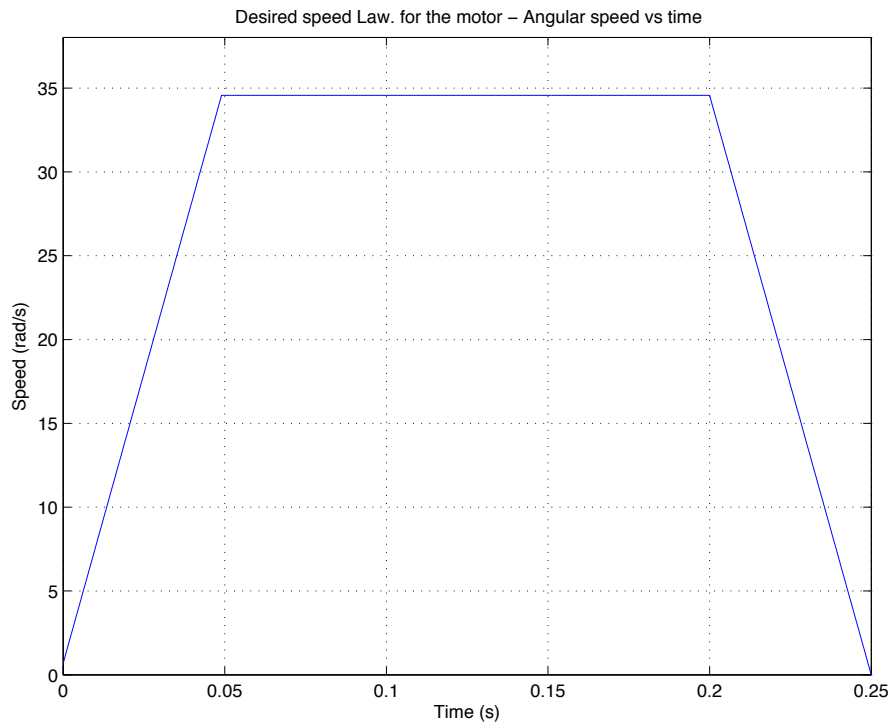


Figure 32: Desired speed law of speed for the motor

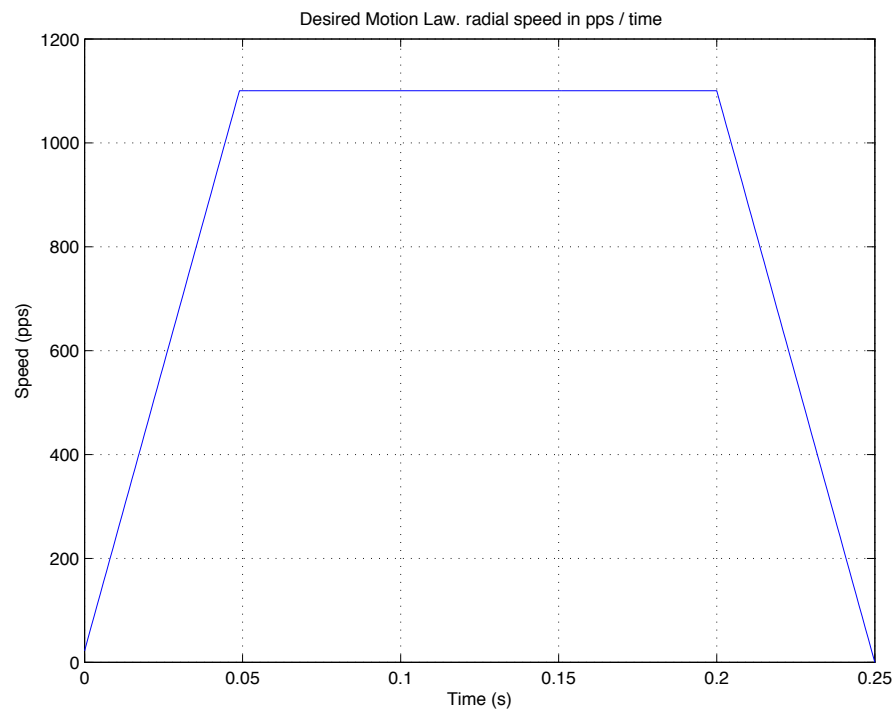


Figure 33: Desired speed law of speed for the motor expressed in pps

3.3.4 Torque required vs time

Given the formulas previously written in this chapter, the trend of the required torque can be analysed. As it can be observed in Fig. 34, the torque required decreases in time because the inertia of the system requires an additional torque during the acceleration but a negative torque when decelerating; as a result, torques values are added with different signs, which produces the curve in Fig. 34.

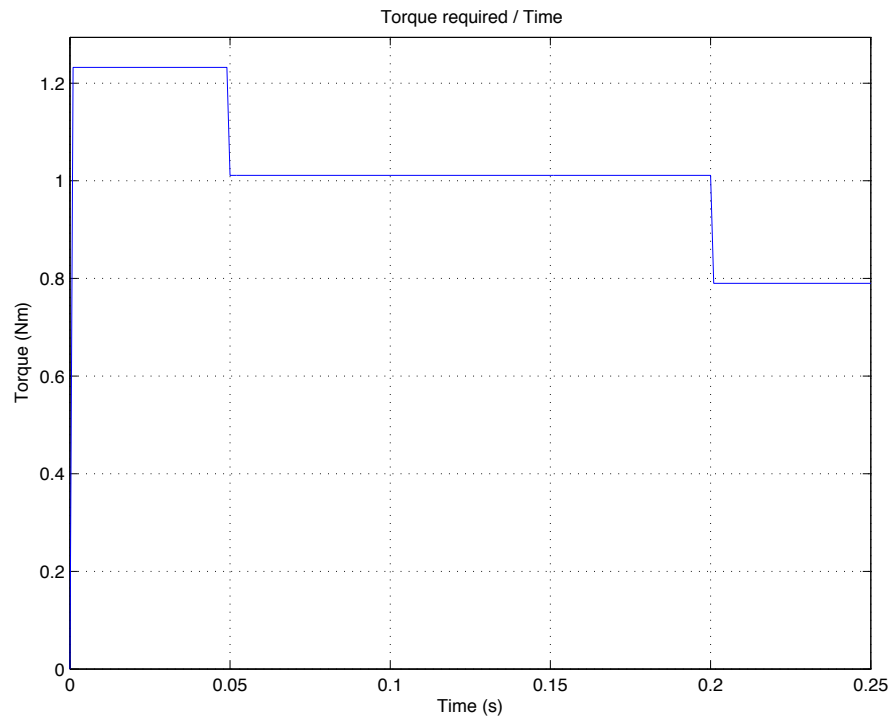


Figure 34: Torque required during the time of the movement

3.3.5 Torque required vs speed

Since the pullout curves are usually expressed in plots with torque values on speed values, it was decided to plot a graphic with the same characteristics, i.e. torque on speed, which can be found in Fig. 35. Since the previous calculations were only done considering the maximum values of torque and speed, the marked point of the plot is the most critical for the entire project, so it was considered first in the calculations. The simulations check how the motor performs in terms of torque and speed during the other phases of the motion. Then, being this a stepper motor, other points must be observed in order to verify, if necessary, the compatibility with the pullin curve. Nevertheless, this curve is not released by the company and so it is assumed that the motor can start in every condition underneath the pullout curve without losing steps.

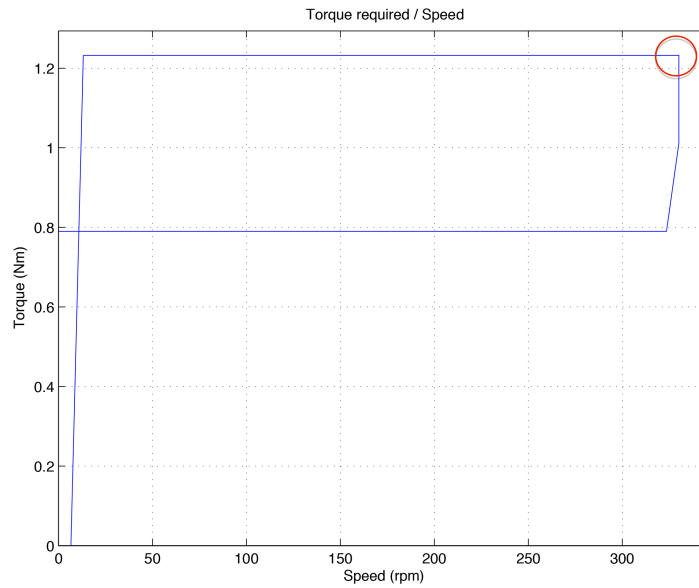


Figure 35: Torque required depending on the speed

3.3.6 Torque required and pullout torque vs speed

As previously said, the required torque curve is compared to the pull-out torque curve and the compatibility is verified. This is shown in Fig. 36.

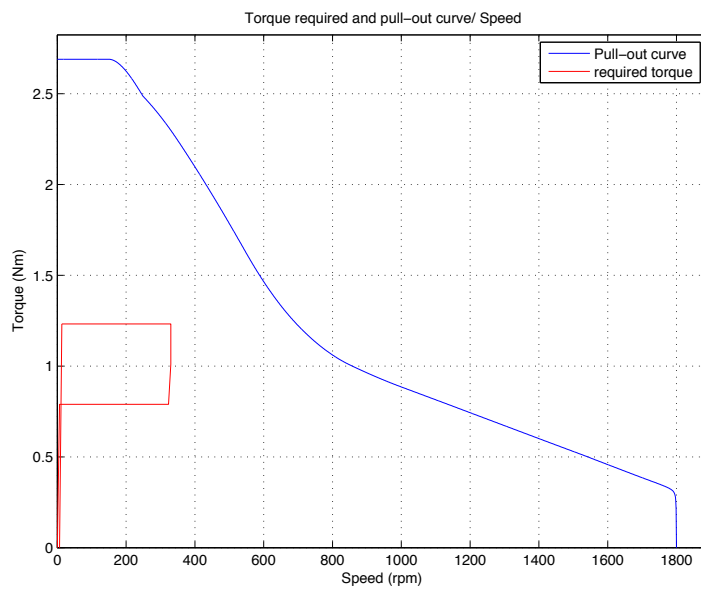


Figure 36: Torque required compared with the pullout torque depending on the speed

3.3.7 Commutation period

Finally, with the simulation, the commutation periods are calculated and some values are represented in Fig. 37. Since the motor does not have a pullin torque, it is to be assumed that it can be started in any condition under the pullout torque. For this reason, given that the speed law has already been decided, the commutation period can be calculated with the commutation frequency, which in turn can be calculated from the speed law. So, in reference to Fig. 33 and through equation 24, the commutation period can be calculated.

$$T_c = \frac{1}{f_s} [s] \quad (24)$$

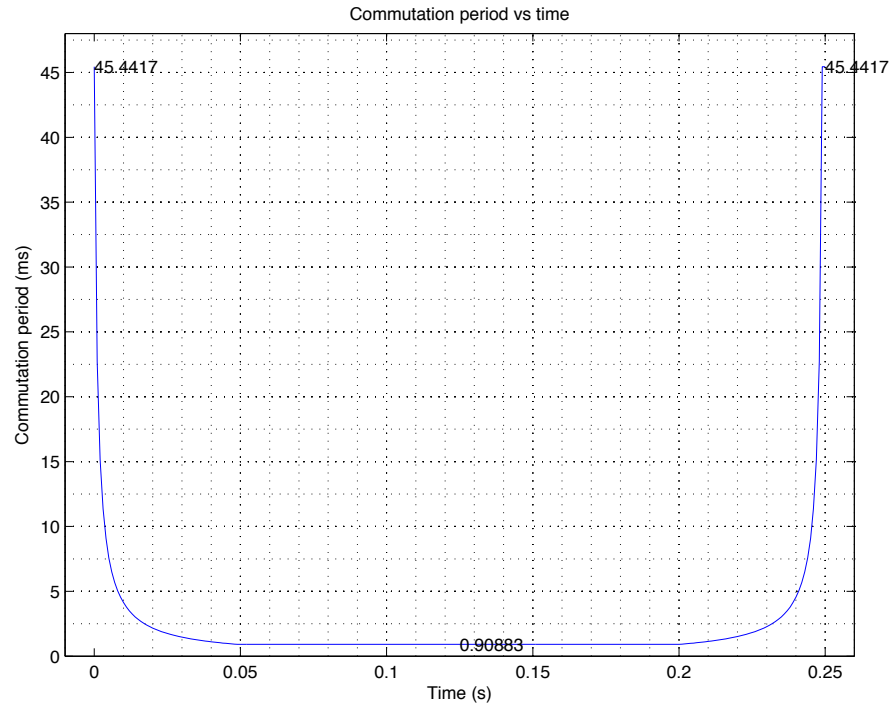


Figure 37: Commutation periods to obtain the desired speed law

BRUSHLESS DC MOTOR SIZING

In order to increase the variety of the solutions it was necessary to change the kind of actuator and it was decided to size a brushless DC motor (BLDCM, in short). This particular motor was chosen because it is a quite good trade-off between weight and nominal power. In addition, the alternatives were an asynchronous motor, a synchronous permanent magnet motor or a common DC motor. The first two kinds of motors were rejected because their implementation requires the use of an inverter. These would imply higher costs as well as more weight, going against the design objectives. Also, the DC motors usually present a lower power density, resulting in an increased weight of the overall system. As a result the sizing of the BLDCM was made for first since it could have led to better results. Nevertheless, given that the BLDC motors are usually made for high speed, the transmission system had to be changed in order to better fit the motor which requires high ratios for the motion completion.

All these considerations led to a new design of the clutch system: it was established that, in order to maintain reliability of the vehicle, an emergency steel lever should be maintained and that lever could be still used for the vehicle start. Despite that, the clutch system was proved to be necessary while downshifting since the driver's "Throttle blipping" is not enough to ensure a reliable gear change. This led to much different scenario for the motor use, since it would only need to operate in a transitory operational mode. So, in the following sections, the BLDC motors will be described and then the calculations will be presented.

4.1 BRUSHLESS DC MOTORS - INTRODUCTION

The Brushless DC Motors are one specific category of the Permanent Magnet Synchronous motors. This categorization is mainly made depending on how the emf (electromotive force, E_d) is applied to the motor itself. In the Brushless AC Motors a sinusoidal wave form of voltage is given to the windings and, by using a control system, the currents are phased with the voltages. On the other hand, the BLDCM are supplied with DC current which is controlled with a switched logic by the control system, usually integrated in the motor itself. This way the motor is fed with emfs nearly squared which are switched from phase to phase in order to allow a synchronous rotation.

These motors are often seen as reversed DC motors since they are built with magnets on the rotor and windings on the stator. As a

result, the brushes can be removed which leads to considerable advantages:

- Longer life.
- Better performance.
- High power density.
- High overcharge capabilities.

4.1.1.1 Structure

As seen in Fig. 38 there are two kind of structures and they differ for the number of poles. In (a) a 2 pole structure is represented while in (b) the motor has 4 poles. These features correspond to a very specific number of phases which are necessary in order to generate the magnetic field which rotates synchronously to the rotor magnetic field produced by the magnets. Referring to the first figure, it can be observed that the rotor is built with a cylinder made of stacked laminations with two curved magnets attached to it. Similarly, the stator is made with stacked and isolated laminations with three teeth facing the rotor. These theets are spaced 120° each other and the copper windings are wound around the teeth in order to create a coil.

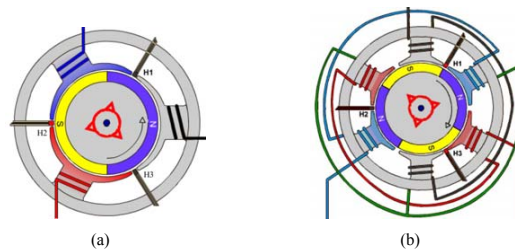


Figure 38: Structure of a Brushless DC Motor. (Courtesy of SERVO MAGNETICS INC, USA)

In the second figure, the 4 pole configuration, the structure is similar but it is improved with the addition of two magnets on the rotor which reflects on 6 stator coils connected in pairs: this design guarantees 3 phases. Furthermore, since the synchronous motors require sensors to properly supply the phases, every teeth of the stator is equipped with a Hall Effect sensor which understands the position of the rotor. By feeding the sensors outputs to the control system, the supply logic can be implemented.

4.1.1.2 Working Principle

The working principle of the BLDC Motor is based on the supply of the stator windings with a nearly squared voltage wave which leads

to a nearly squared current wave conveniently synced with the voltage. These currents, in turn, produce a magnetic field which interacts with the magnetic field produced by the rotor magnets is common in the electrodynamic systems. The emf and current waveform can be observed in figure 39.

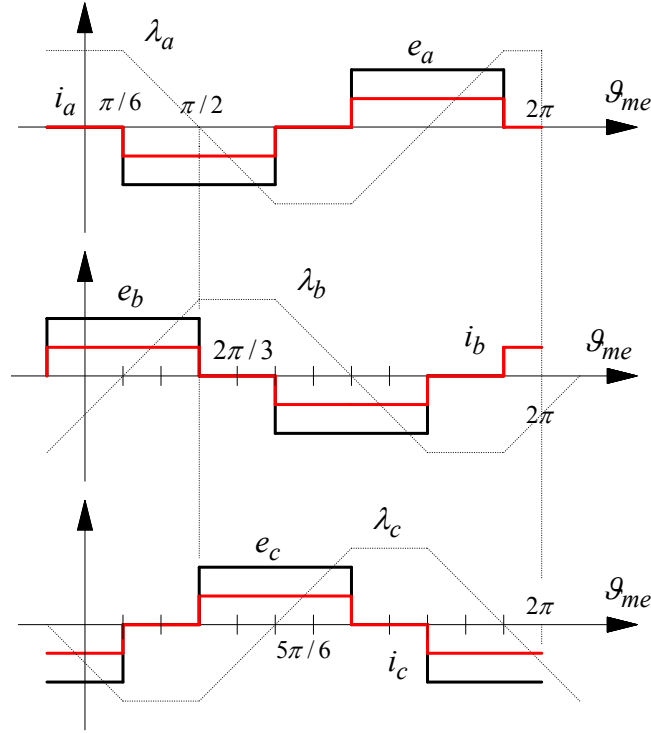


Figure 39: Working principle of a BLDCM Motor. [4]

The force produced by the interaction of the two magnetic fields makes the rotor to turn: however, the torque generated by the motor is not continuous since the phases are placed every 120° so every commutation is made every 60 electrical degrees: this leads to a step-like movement. As a result the output torque will present a small ripple which can be ignored while the motor is spinning.

4.2 REVISED TRANSMISSION SYSTEM

As said in section 2.4, the solutions for the transmission systems can be numerous and each one must be considered with the motor. In chapter 3, since a stepper motor was used, a ball screw could be used: this was possible because stepper motors usually have an high stall torque at low speeds but this torque decreases quickly with higher speeds, so a low gear ratio was needed. On the other hand, BLDC motors are made for high speed and since the clutch actuation requires a high torque it is necessary to use high gear ratios. This reduced the design possibilities of the transmission, forcing the use of a planetary

gearbox with high reduction ratios which, in turn, implied to position the motor and the gearbox connected axially to the clutch. This solution is quite complex to implement because it forces the clutch motor to be positioned vertically above the clutch lever but, since the BLDC motors usually have an higher power density, they are smaller than stepper motors. So, in conclusion, this solution was considered to the best trade-off between weight and performance of the solution.

4.3 BLDCM MOTOR SIZING

When the sizing was firstly approached an issue raised: since the actuator is supposed to be placed on a FSAE vehicle, a lot of care must be taken while sizing a motor. In fact, in a motorsport-like environment, performance plays a great role and weight is an always present enemy. So, the commonly used practice of doubling the torque requirements as safety procedure was rejected because it would lead to a heavy design. In addition, as said in the beginning of this chapter, the motor is supposed to work with intermittent repetitions of the speed law.

All these considerations led to the conclusion that in order to exactly determine if a particular motor is suitable for the application, a thermal simulation had to be made. Obviously, the rated power parameter given in every BLDCM datasheet is referred to a continuous operation which does not reflect what is required to the clutch actuation system.

So, in order to better estimate how a motor would behave when used in a very specific environment, a thermal model was developed and implemented with a Matlab script. These two topics will be presented in the following section.

4.3.1 *Thermal model*

As said before, the thermal design was chosen to be the best way to correctly estimate the behaviour of the motor and to better size the motor. The common literature usually models the motor with one single thermal resistor and, sometimes, with one capacitor. However, that model is only appropriate for continuous operation modes and does not fit properly the intermittent operation mode. Moreover, since the overall design goal is to save weight, it was decided to choose an undersized motor because of the operation mode it is supposed to have. So, it was necessary to build a better thermal model, which was found in Maxon Motor's Formulae Handbook [1]. In this document a model is presented where the heat is produced by different sources such as iron losses, friction losses due to the bearings and

Joule effect losses. Nevertheless, the main cause for heat production is the Joule effect given by the following formula.

$$P_j = R_{Tw} \cdot I_{mot}^2 \quad (25)$$

The terms in equation 25 are:

- P_j : Joule power losses in winding.
- R_{Tw} : Winding resistance based on current winding temperature T_w .
- I_{mot} : current flowing through the winding.

As a matter of fact, R_{Tw} changes with the temperature and this was found to be a quite difficult problem to solve when implementing the Matlab script because it varies with the following equation:

$$R_{Tw} = R_{mot} \cdot [1 + \alpha_{cu} \cdot (T_w - 25^\circ\text{C})] \quad (26)$$

The terms in equation 26 are:

- R_{mot} : Resistance at ambient temperature.
- α_{cu} : Resistance coefficient of copper.
- T_w : current winding temperature.

Since the calculation of the winding temperature is the main goal of the whole process, the dependency of the power from the temperature imposed a complication in the overall calculation but it was solved in the Matlab script. As said before, the model implemented takes into account the thermal resistance of both the winding-housing part and the housing-ambient part. This allowed a more precise model to be created. As shown in figure 40, the model implemented is based on an analogy to an electrical circuit. In this model, the thermal resistance is modelled with a resistor and capacitors are added in order to model the time required for the heat to dissipate. Also, the power to dissipate is linked to the current entering the circuit and, finally, the voltage drop is associated with a temperature gap. So, having separated the winding-housing from the housing-ambient resistance, the model is built with current flowing through the four components. By calculating the voltage drop on the resistors the temperature drop can be calculated and so the motor can be sized.

Thanks to this model, the problem became electrical so the voltage was considered as system output, the current the system input and the equivalent impedance calculated with the Laplace transform resulted to be the transfer function of the system. This was used in the Matlab script in order to estimate the peak temperature of the motor.

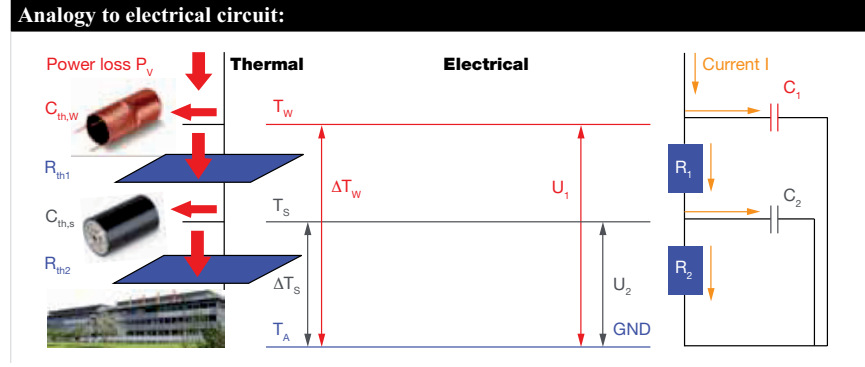


Figure 40: Electrical-thermal model. Image courtesy of Maxon Motors.

Given the circuit represented in figure 40, the following mathematical calculations were used:

$$V = Z_{eq} \cdot I \quad (27)$$

As said before, Z_{eq} is the transfer function of the system and it can be called W and, in equation 27, V is the voltage drop on the two resistors. In addition, Z_{eq} can be written as follows:

$$Z_{eq} = (Z_{R1} + Z_2) \parallel Z_{C1} \quad (28)$$

In particular, the terms are:

- $Z_{R1} = R1 = R_{th_{winding}}$: Thermal resistance between winding and housing.
- $Z_{C1} = \frac{1}{sC_1}$: Impedance of the winding capacitor.
- $Z_2 = Z_{R2} \parallel Z_{C2} = \frac{R_2}{1 + C_2 R_2 s}$: Impedance of the parallel of the resistance and capacitor between housing and ambient.

By substituting the terms in equation 28 and with some mathematical calculations, the transfer function can be written as follows:

$$W = Z_{eq} = \frac{Z_{C1}R_1 + Z_{C1}Z_2}{Z_{C1} + R1 + Z_2} \quad (29)$$

After that, by using the command “Isim” in Matlab it is possible to use an input signal to simulate the time domain response of the dynamic systems to arbitrary inputs which is exactly what is needed.

So, in order to determine whether a motor is suitable for this particular application or not the following procedure was used:

- The motor is selected from numerous websites considering the rated power it can supply.
- A first Matlab script is executed and an optimization of the gear ratio is made.

- By analysing the feasibility of the ratios and by comparing the values with the company's catalogue, a gear ratio is chosen.
- A second Matlab script is executed which completely simulates the working cycle of the motor. This is done by using some logged data collected during a race of the MG0914.
- The maximum temperature reached is compared with the maximum allowed temperature and then a safety factor is calculated in order to compare different motors.

In the following sections the Matlab script is explained thoroughly since it is vastly used for the motor sizing. After that, the simulation results will be used for the motor comparisons.

4.3.2 Matlab scripts

The first Matlab program is based on an evolution of the program presented in appendix A. Starting from the desired speed law, some ratios are continuously changed and, in every loop, the desired speed law is reflected on the motor and, then, the torque is calculated. After that, through the torque constant, the required current is calculated. This single load cycle must be applied to a real case scenario so, in order to do that, the data acquisition software of the MG0914 was used to extract a .mat file which contains a vector of the down shift requests. A brief introduction on the data acquisition system of the vehicle can be found in appendix B. By overlapping a load cycle to every down shift request it was possible to determine a current signal needed for the thermal calculations.

Then, by using the command "lsim" in Matlab it was possible to estimate the peak temperature reached during the race and, by looping the entire program for different gear ratios, it was possible to find a relationship between peak

Figure 41: Graphical user interface used for the Matlab scripts.

temperature in function of the ratio. By using this information alongside with the maximum gearbox input speed, it was possible to find the best trade off in order to save weight. After the ratio selection, an evolution of the Matlab script was made in order to deeply analyse the temperature trend during the race and to monitor every parameter of the load cycle.

So, in the following sections, these two scripts are used for every motor and the following plots are produced:

- Peak temperature vs ratio: this plot is used to choose the best gear ratio.
- Temperature vs time: this plot is used to understand the winding temperature trend during the race.

After that, a safety factor is calculated with this formula:

$$\nu = \frac{\Delta T_{\max}}{\Delta T_{\text{motor}}} \quad (30)$$

- ΔT_{\max} : It is the maximum allowed temperature rise.
- ΔT_{motor} : It is the maximum temperature rise reached by the specific motor.

As said in the beginning of this work, the different motors will be compared using the safety factor and the weight. In the following subsection some BLDC motors will be analysed, but they will be picked from only two companies, Maxon Motors and Faulhaber because those two companies are the only one who report the thermal data required by the Matlab scripts. It must be noted that it is assumed to work in a quite hot environment, i.e. near the engine itself, and since the hot temperature of the internal combustion engine, we assume a working temperature of 55 °C. This is used to set the reference level of the simulation. The two scripts can be found in appendixes [C](#) and [D](#). In the following sections each motor will be analysed and it's behaviour will be simulated. Moreover, all the following motors are built for a 12 VDC power supply and this is common to every motor.

4.3.3 *Faulhaber 3056 K 012 B*

The first motor analysed is the Faulhaber 3056 K 012 B, which is a 48W rated power motor. From the first Matlab script it emerges that, as it can be observed in figure [42](#), the optimal ratio is about 650. Despite that, by running a complete simulation with that ratio, the temperature trend clearly shows that the motor being considered is not sufficient for the motion completion. Moreover, a gear ratio of 650 is not allowed by gearboxes of the same company, since the maximum

input speed allowed for the gearbox is about 4500 rpm. By attempting to choose a proper ratio to satisfy the input speed requirement, the simulation diverges because the loop used to calculate the motor phase-to-phase resistance variation depending on the temperature diverges.

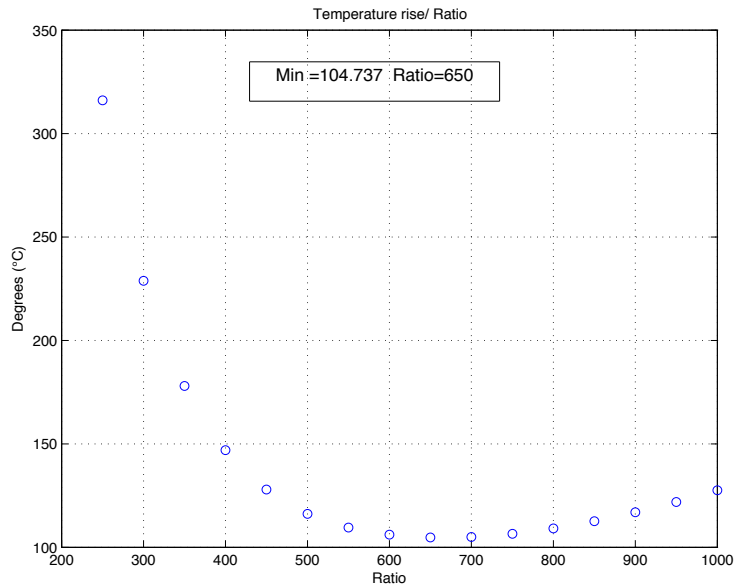


Figure 42: Peak temperature vs ratio.

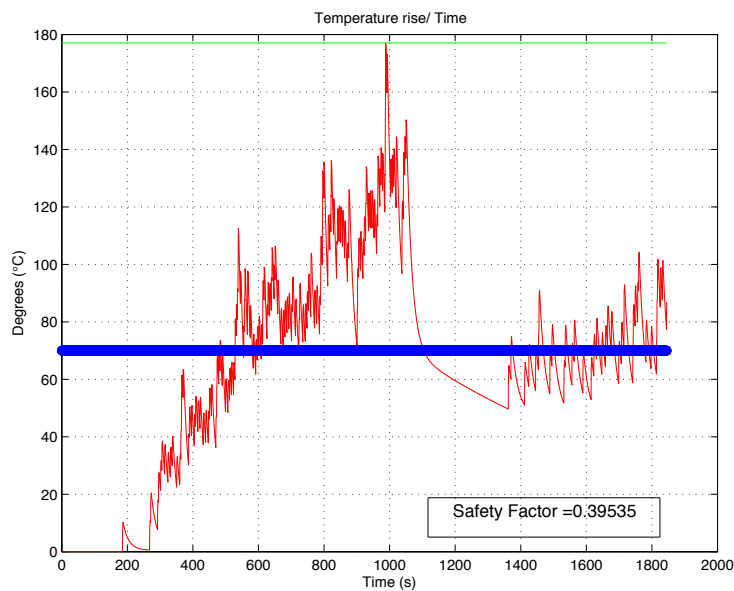


Figure 43: Temperature raise vs time. Ratio 650.

4.3.4 Faulhaber 2057 S 012 B

The second motor analysed is the Faulhaber 2057 S 012 B, which is a 61W rated power motor. Following the same steps of the first motor, a new temperature vs ratio plot was made and, as it can be observed in figure 44, it was observed that the optimal ratio is about 1050. Despite that, by running a complete simulation with that ratio, the temperature trend clearly shows that the motor being considered is not sufficient for the motion completion. As the first motor, a gear ratio of 1050 is not allowed by gearboxes of the same company, since the maximum input speed allowed into the gearbox is about 4500 rpm. By attempting to choose a proper ratio to satisfy the input speed requirement, the simulation diverges because the loop used to calculate the motor phase-to-phase resistance variation depending on the temperature diverges.

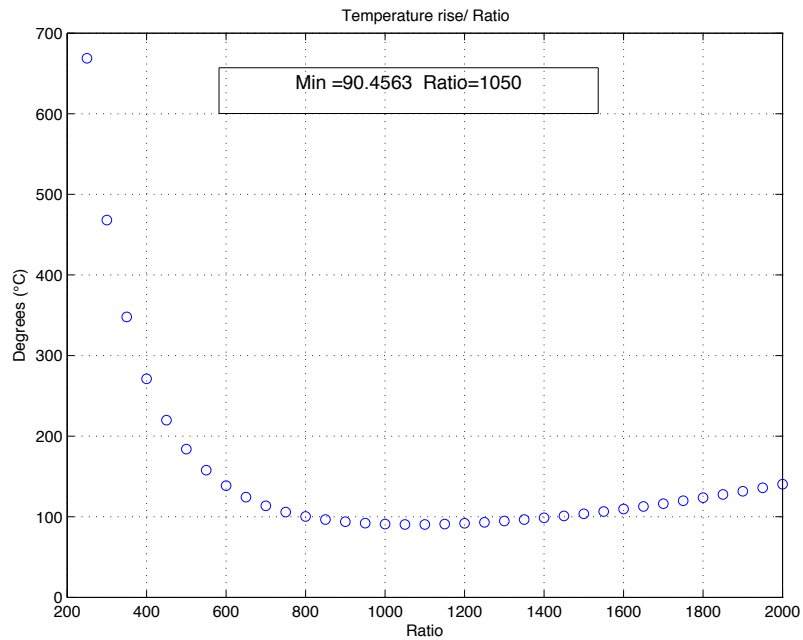


Figure 44: Peak temperature vs ratio.

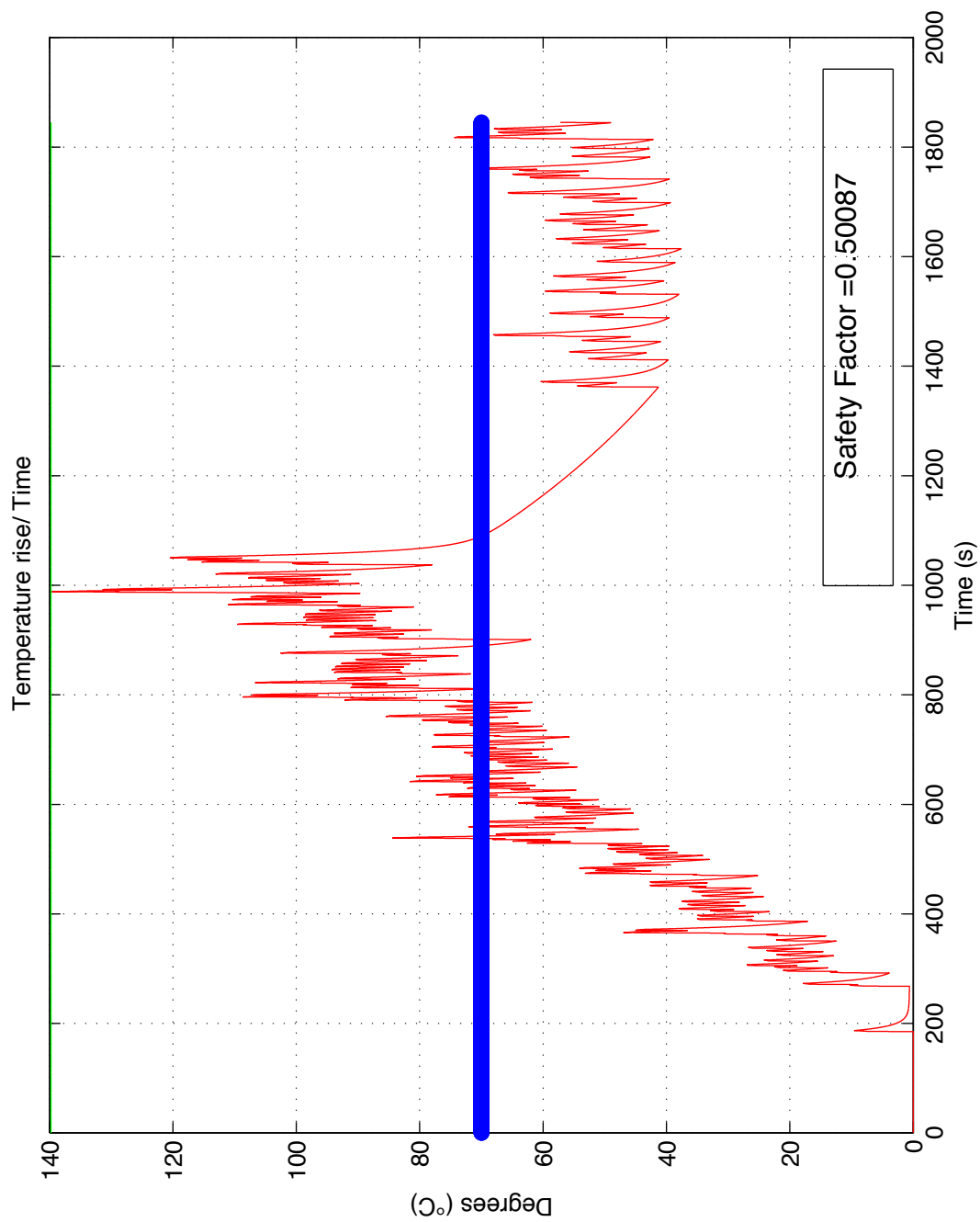


Figure 45: Temperature raise vs time. Ratio 1050

4.3.5 Faulhaber 3564 K 012 B

This motor, the last from Faulhaber, is the Faulhaber 3564 K 012 B, which is a 109W rated power motor. The first Matlab script plotted some interesting results since the optimum ratio was quite lower if compared to the following two motors. This, in fact, is an advantage considering that the Faulhaber gear ratios require low input speed so. The results of the gear ratio optimization can be observed in figure 46 As seen in figure 47, the simulation was made with the optimum ratio of 400. In this case, the motor fits the requirements and it has a safety factor of:

$$\gamma = \frac{\Delta T_{\max}}{\Delta T_{\text{motor}}} = 1.336 \quad (31)$$

This could be a viable solution for the problem being studied, and the motor would be used quite on the edge. Nevertheless, this gear ratio requires a very high speed to the motor which does not fit any gear ratio. So, the simulation had to be made again with a lower ratio, in order to fit this particular requirement. The simulation results can be observed in figure 48 and it can be seen that, with a gear ratio of 150, the motor is not able to fit the requirements and it would result in a breakdown.

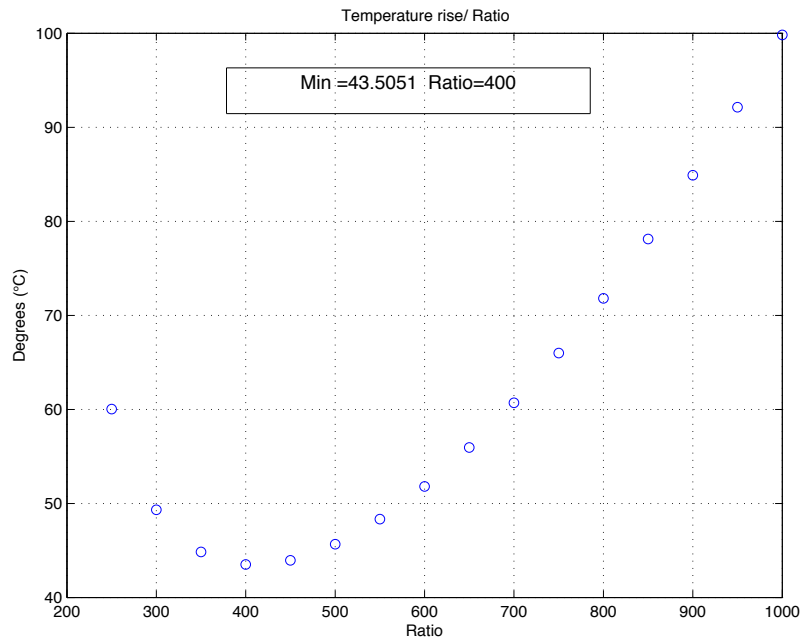


Figure 46: Peak temperature vs ratio.

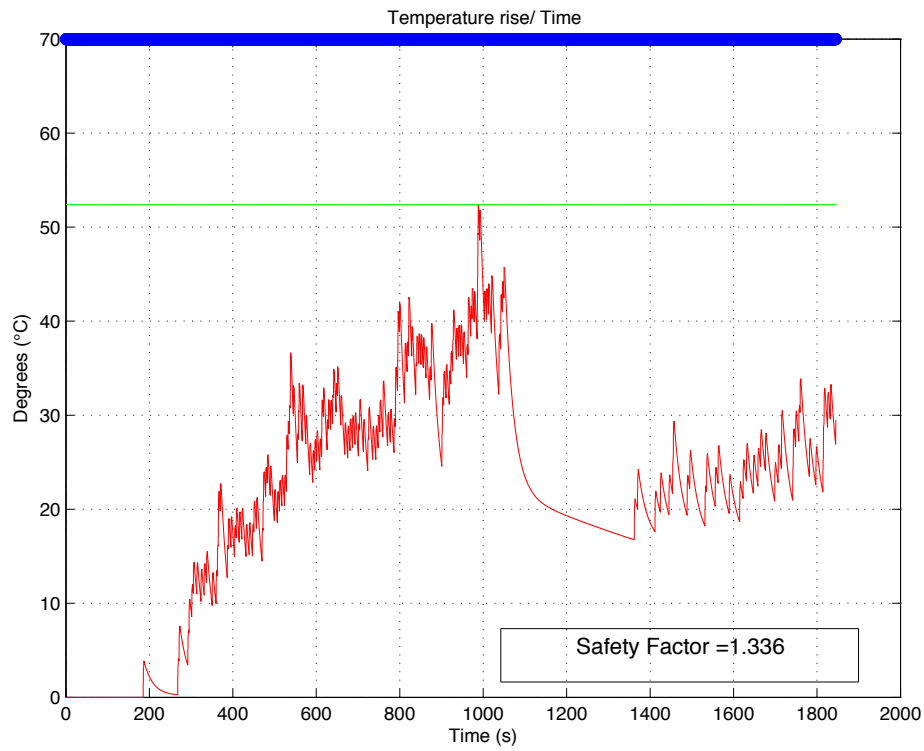


Figure 47: Temperature raise vs time. Ratio = 400.

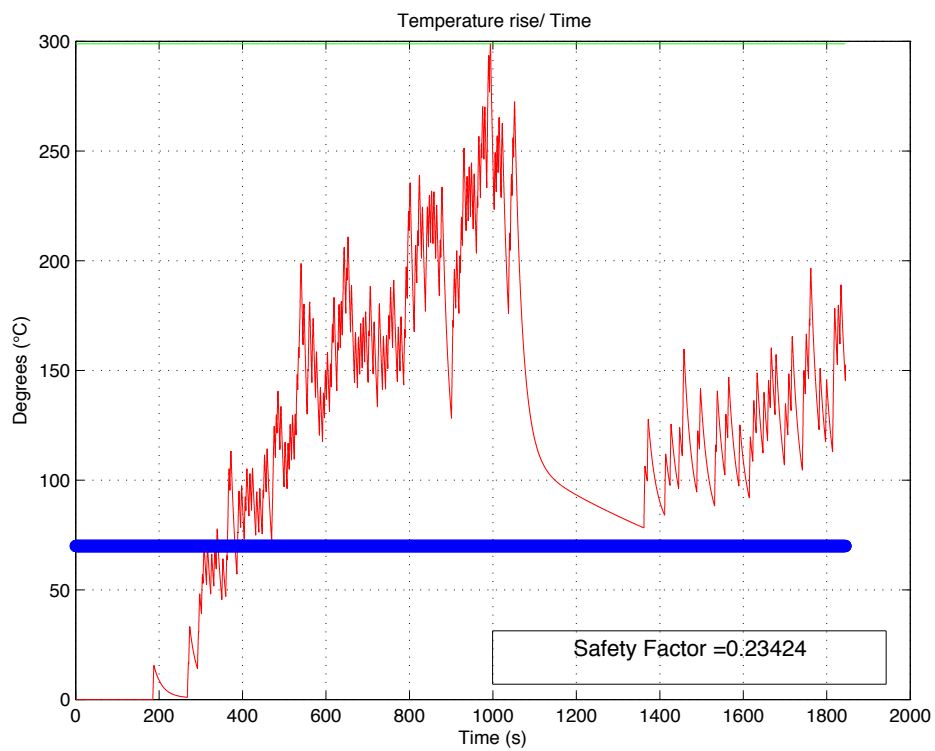


Figure 48: Temperature raise vs time. Ratio = 150

4.3.6 Maxon Motor EC-max 30 40 Watt

After considering three motors from Faulhaber, the focus switched to another company: Maxon Motors. Despite changing company, the scripts were used in the same way in order to be able to compare the results. So, the first motor analysed was the EC-max 30 from Maxon Motors, which has 40 Watt of rated power. The first simulation's result is represented in figure 49 and it can be observed that the optimal gear ratio is 700. After that, the second simulation was made, using 700 as ratio and the results were quite impressive: as it can be noted in figure 50, even if the rated power is less than the mechanical power required, it seems like this motor could fulfil the requirements with a safety factor of 1.8402. Nevertheless, as for the Faulhaber 3564 K 012 B motor, the gearbox must be considered. However, Maxon Motors' gearboxes are built for higher speeds and they allow input speeds up to 8000 rpm. This favours the motor sizing, allowing greater reduction ratios and better use of the motor. So, as a result, a final simulation was made with a gear ratio of 275 which proved this motor to be inadequate for the task because the peak temperature rises too much. This result is represented in figure 51.

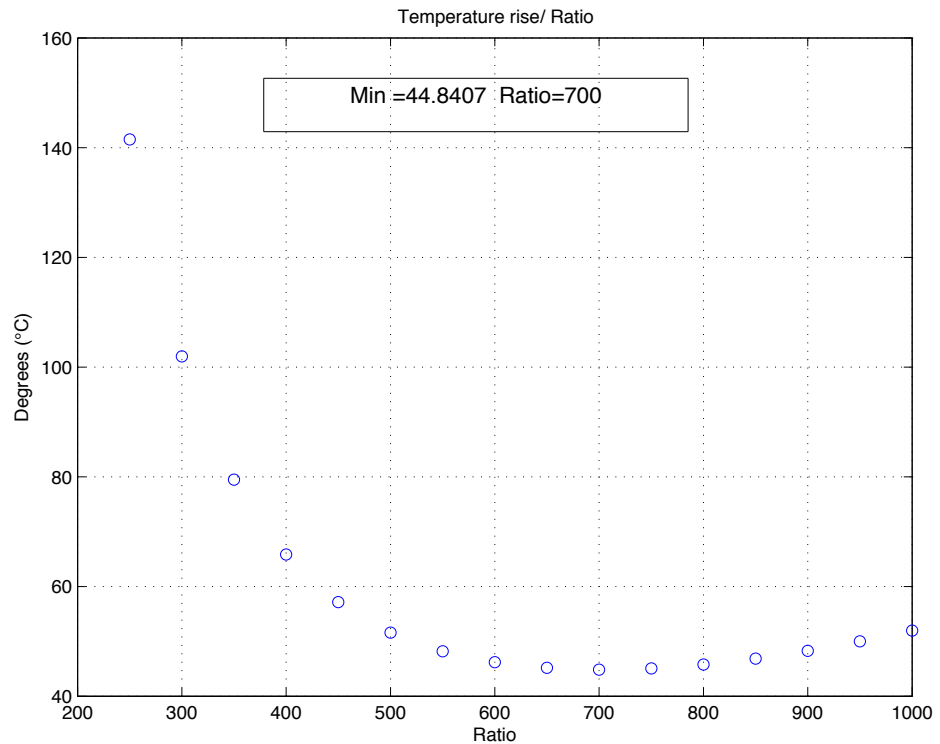


Figure 49: Peak temperature vs ratio.

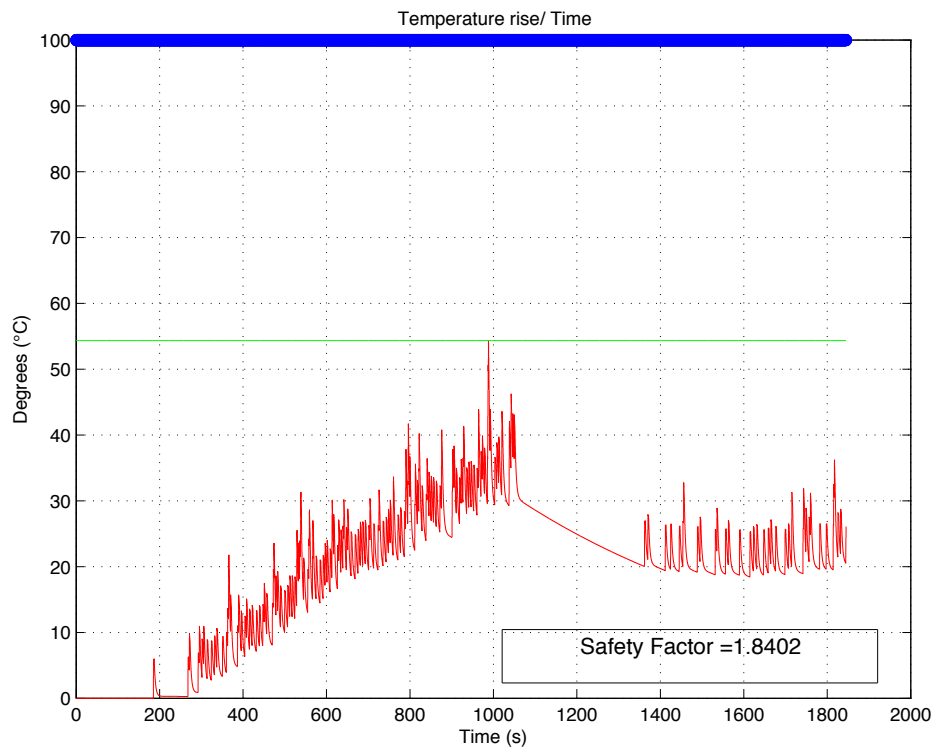


Figure 50: Temperature raise vs time. Ratio 700.

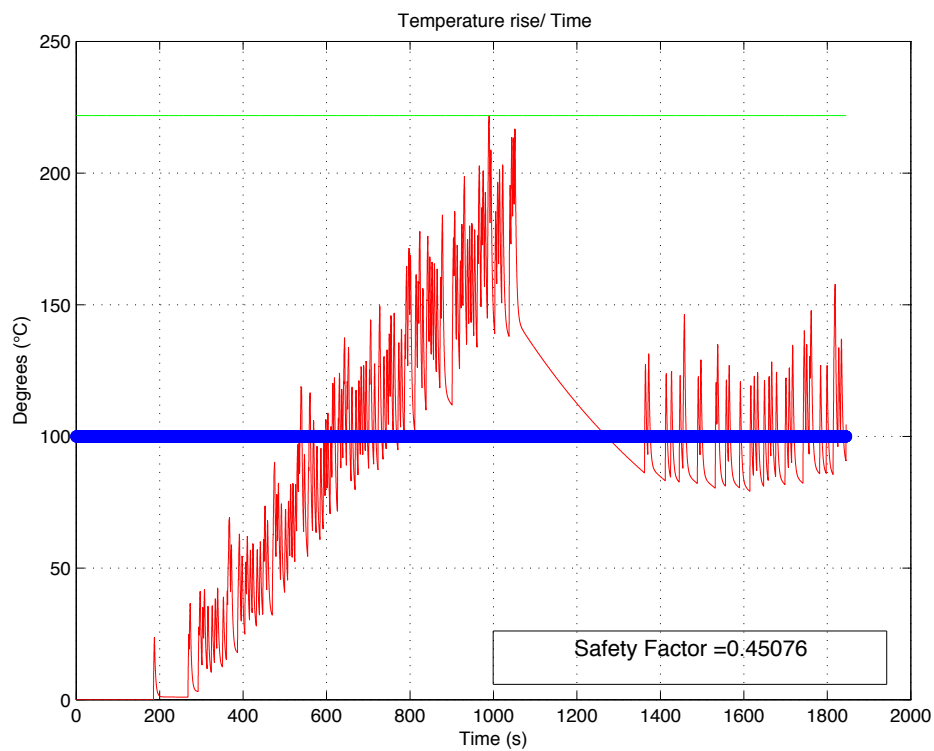


Figure 51: Temperature raise vs time. Ratio 275.

4.3.7 Maxon Motor EC-i 40 50 Watt

After the 40 W motor, the EC-i 40 with 50 Watt of rated power was analysed. As always, the BLDCM ratio.m script was run for first and the optimal ratio was found at 700. So, the complete simulation was made with that particular ratio and a safety factor of 3.7795 emerged and it can be seen in figure 53. Also, the maximum temperature raise is about 27°C which, added to the 55 °C of the working temperature, sets the peak temperature to 82°C. This is quite a good result, especially given that this motor is quite small and it weighs only 170 grams.

However, as said before, a ratio of 700 is not suitable to the common gearboxes so a ratio of 285 was used for the second simulation and the results are presented in figure 54. This simulation shows that this motor would be perfect in this particular condition. Nevertheless, care must be taken because using a safety factor of 1.0693 requires to have very precise data and a very precise use of the electric drive. Since the torque requirements were made with a quite imprecise method, there is not confidence enough to accept this result. In fact, the 285 ratio was chosen from Maxon Motor's catalogue and it was chosen in order to fulfil the input speed requirement.

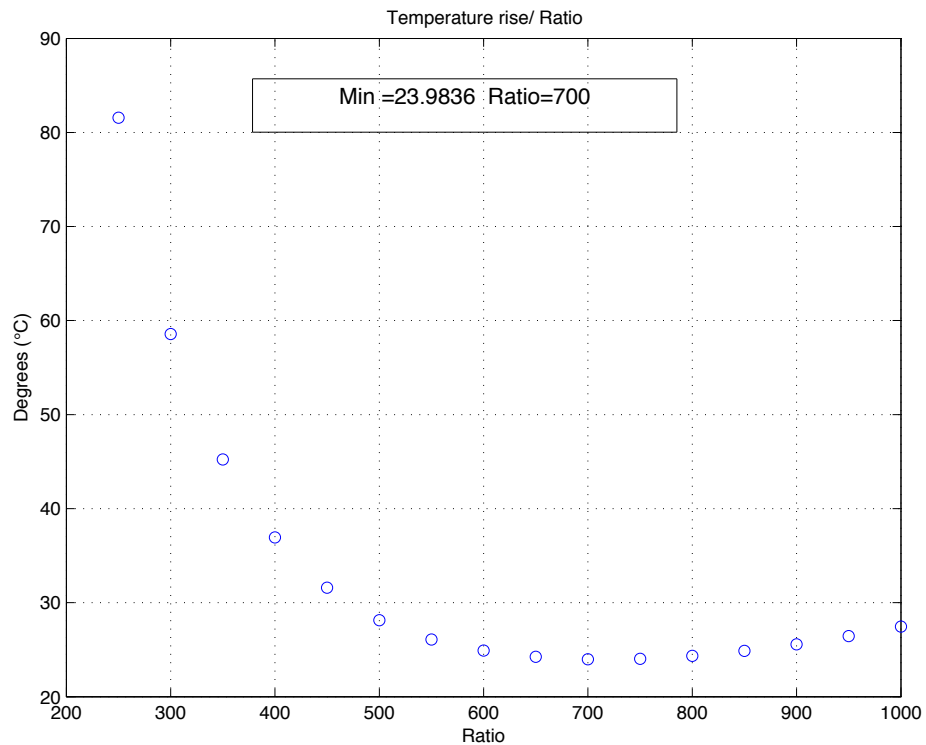


Figure 52: Peak temperature vs ratio.

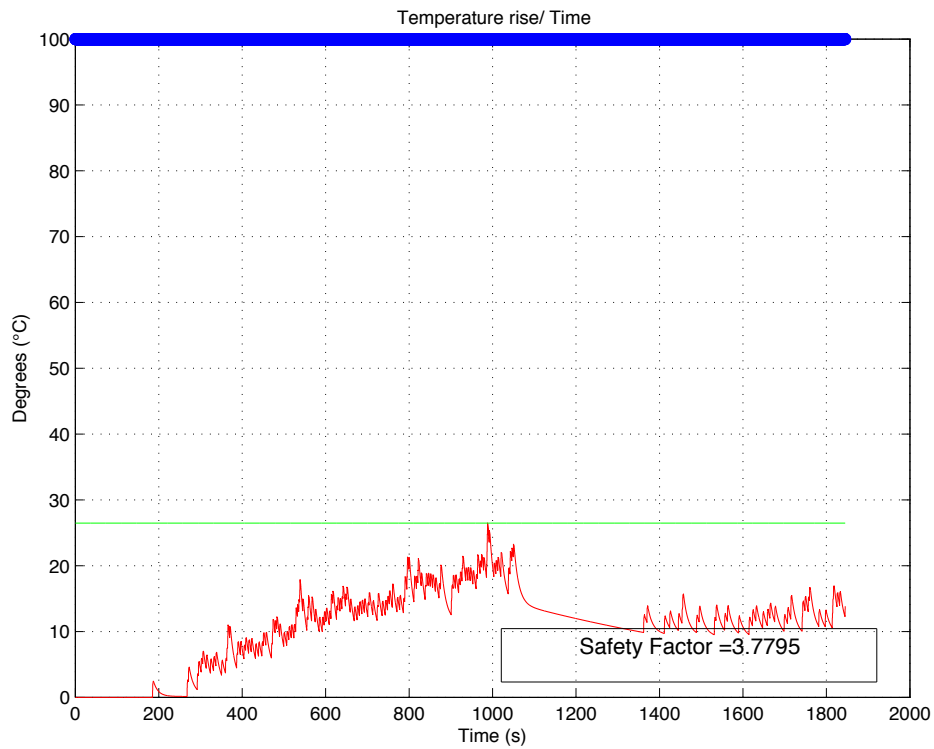


Figure 53: Temperature raise vs time. Ratio 700.

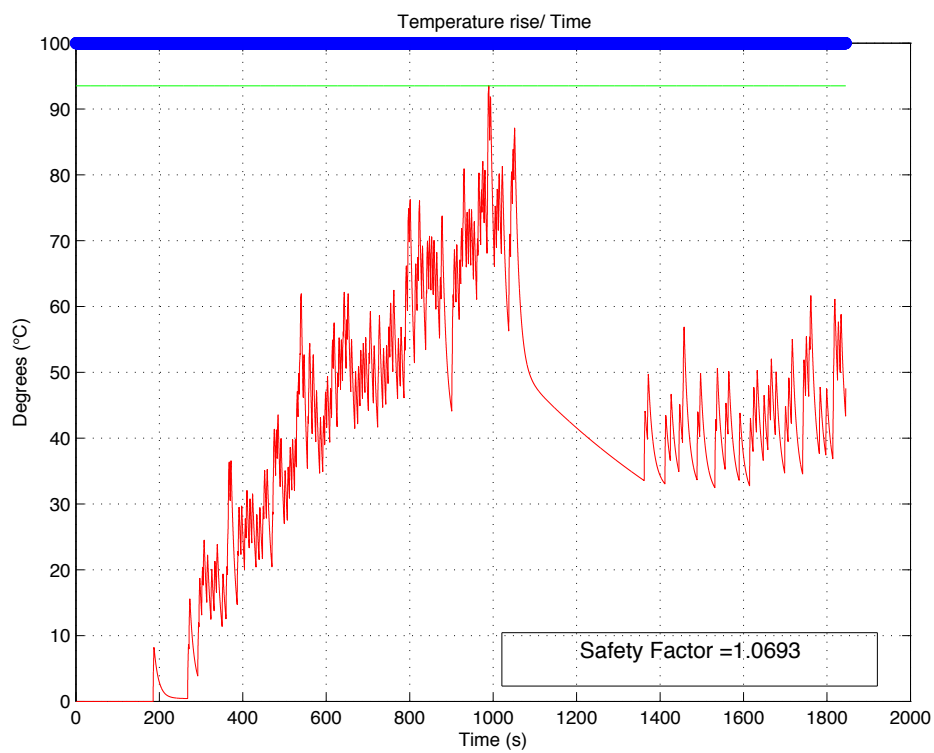


Figure 54: Temperature raise vs time. Ratio 285.

4.3.8 Maxon Motor EC-max 30 60 Watt

The last motor being considered is the EC-max 30 with 60 W of rated power. This motor is the most powerful of the Maxon Motors motors considered until this point. The first Matlab script gives figure 55 in return where it can be noted that the optimum ratio is 500. After simulating the optimum ratio, a ratio of 257 was simulated since it allows the input speed of the gearbox requirement to be respected and also to use the gearbox more efficiently. The simulation, made with parameters of real components, gives figure 57 as a result. The numeric values of this simulation are:

- Top speed required to the motor = Top input speed of the gearbox = 7282 rpm.
- Peak torque required to the motor = 132.2 mNm.
- Peak current absorbed from the motor = 9.31 A.
- Root mean square of the current adsorbed = 2.83 A.
- Peak winding temperature during the race = $41.1\text{ }^{\circ}\text{C} + 55\text{ }^{\circ}\text{C} = 96.1\text{ }^{\circ}\text{C}$.
- Safety factor = 2.4334.
- Overall weight = 860 grams.

Since the safety factor found is 2.4334, it is considered a sufficient value that guarantees the best trade-off between performance, weight saving and reliability.

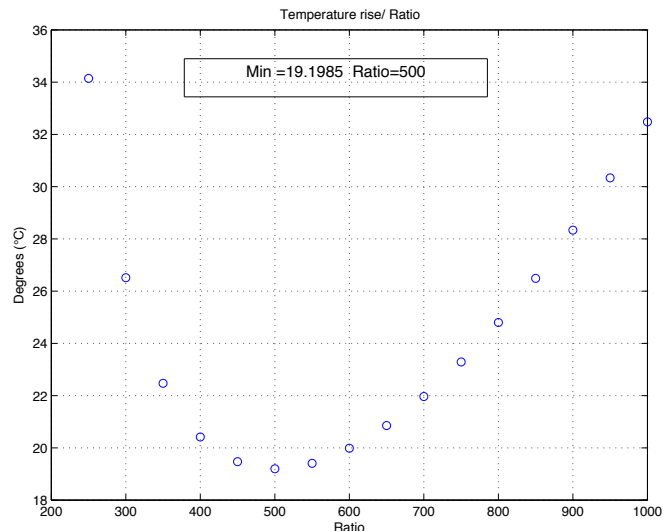


Figure 55: Peak temperature vs ratio.

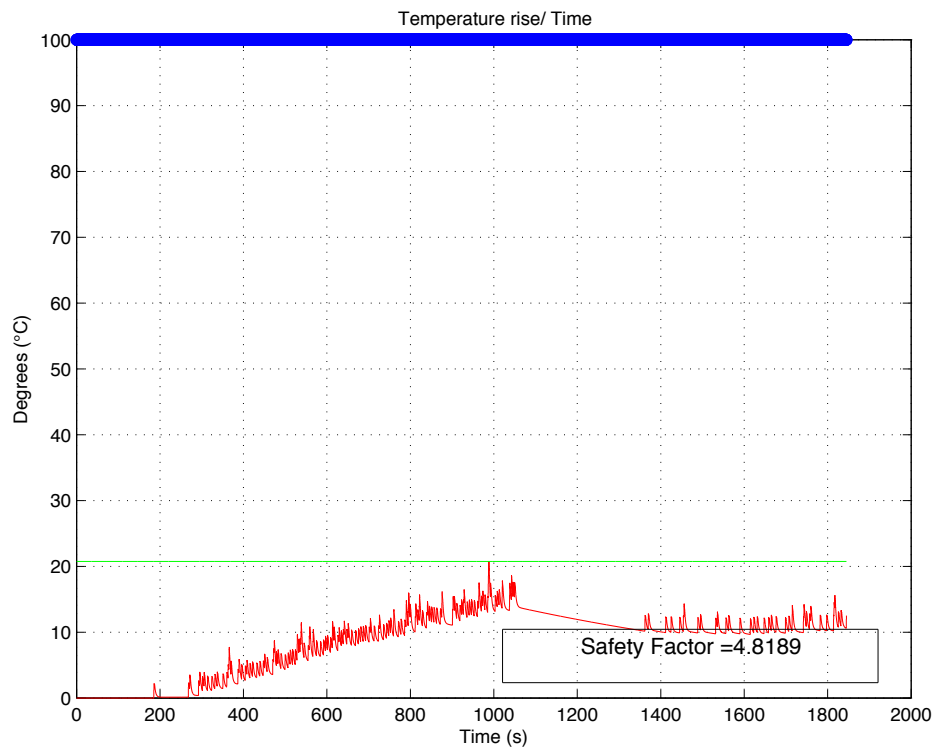


Figure 56: Temperature raise vs time.

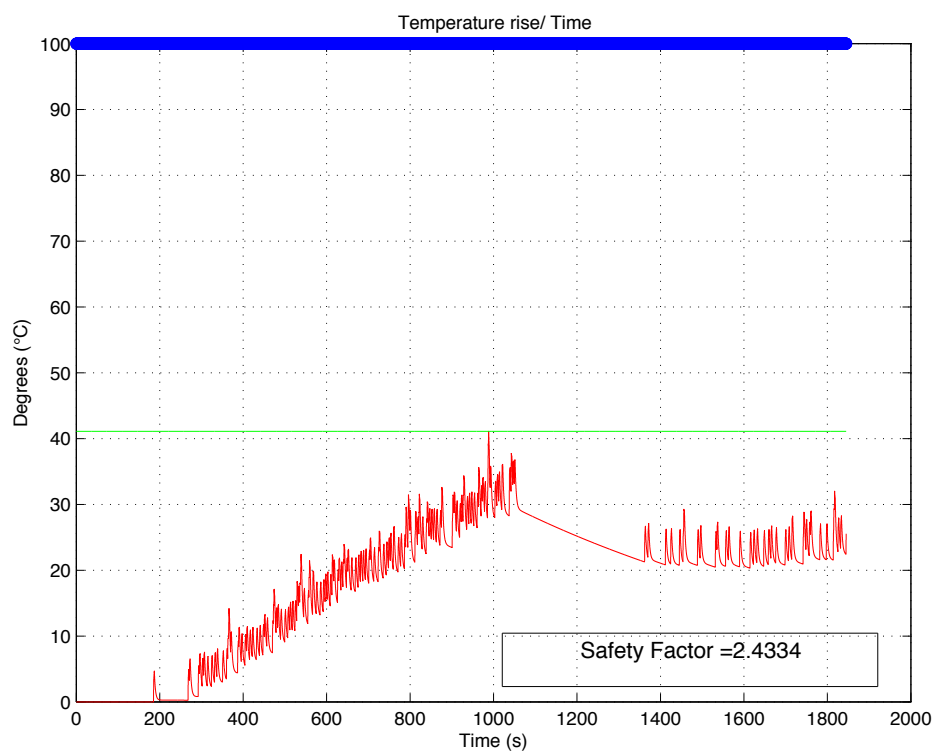


Figure 57: Temperature raise vs time.

CONCLUSION

The aim of this chapter is to revise the whole analysis and to discuss the results in order to consider the real implementation of the electrically-actuated clutch on the future single-seat car of the Race UP Team, the MG X-15. The aim of this script is to prove the feasibility of an electrically-actuated clutch for a FSAE vehicle. In the first part the torque and speed requirement were experimentally extrapolated with an experiment. Despite some precautions were taken in measuring the force, the experiment was made on a workshop bench with a still engine. These measurements should include the inertia of the clutch system starting from the gear clutch lever: nevertheless, it is an assumption made and it needs validation.

In addition, nothing has been said about how the clutch lever disconnects the internal engine shafts: this means that the clutch lever could move for a lower angle and still complete the task. In fact, to obtain this information, a force sensor should be applied between the steel cable and the clutch lever in order to verify how the clutch behaves depending on other variables.

Also, the calculations were made with self-developed Matlab scripts which solves a model and a self-made Excel file. Also, the thermal-electrical model described in section 4.3.1 must be validated in order to understand the relationship between the model and the reality. A good way to analyze the model could be to attach some masses to the motor and measure the current adsorbed by the motor when controlled to execute the designed law of motion.

In conclusion, it must be noted that nothing has been said about the control of these actuators, which is a very important aspect that deeply influences the final choice. The ease to implement a control system and its weight were not taken in consideration as they should have, especially if thinking about an implementation of the system. As a matter of fact, in order to save time and to make a simpler system, a DC servomotor could be used since they integrate a ratio as well as a closed loop position control system.

Finally, since two kind of motors were analysed, a comparison is needed: the best stepper motor found was the HT34-504 with a total weight of 1.59 kg. Also, the ball screw must be added, so the total weight should be about 2 kg. The BLDCM solution, on the other hand, only weighs 860 g. In addition, the HT34-504 motor requires a 24V supply, which requires a boost converter in order to amplify the 13V available on the vehicle. So, for these reasons, the BLDCM

is considered to be the best fit for the application, with a thorough validation of the model.

APPENDIX A - MATLAB®

The aim of this appendix is to report the MATLAB® code used for the simulation of the motors. This way, the reader can better understand the reasoning behind the simulation. Also, the code is offered so that the reader can copy and paste it and execute it.

```
%Torque calculation and HT34-504 simulator

%% ENVIROMENT PREPARATION
close all;
clear all;
clc

%% MOTOR PARAMETERS
Jm = 1.1*10^-4; % motor inertia [kg*m^2]
Np = 200; % steps number for one revolution
alfa_p= 2*pi/Np; % step angle [degrees]

%% BALL SCREW PARAMETERS
Jv = 2.10*10^-4; % screw inertia [kg*m^2]
lead = 0.03; % righ hand lead [m]
r_eq = lead/(2*pi); % equivalent radius [m]
efficiency = 0.85;

%% SYSTEM REQUIREMENTS
F = 270; % Force necessary to move the load. [N]
time_total = 0.25; % total time to move the load. [s]
time_rise = 0.2*time_total; % Time in which the load accelerates. [s]
movement_angle = 34; % degrees of engine clutch lever movement
movement_angle_rad = (movement_angle*pi)/180;
mean_angular_speed = movement_angle_rad / time_total;
speed_medium = (mean_angular_speed * 0.037) + 0.0002; % linear and medium speed of the load
% compensated for truncation.
speed_peak= (speed_medium*time_total)/(time_total-time_rise); % top linear speed. [m/s]
radial_speed_peak = speed_peak/r_eq; %top radial speed reached by the motor [m/s]
TL = (F*speed_peak)/(radial_speed_peak*efficiency); % Load Torque

time = [0:0.001:time_total]; %Time vector
[uno, samples] = size(time); %Number of time units

%% DESIRED MOTION LAW PLOT
% In this section the plot for the desired motion is implemented

CODE REMOVED FOR PUBLICATION PURPOSE
CONTACT marcozorzi@icloud.com FOR THE ORIGINAL CODE

%% DESIRED MOTION LAW PLOT FOR THE MOTOR
% The desired motion law is transferred to the motor through the ball screw

CODE REMOVED FOR PUBLICATION PURPOSE
CONTACT marcozorzi@icloud.com FOR THE ORIGINAL CODE

%% DESIRED MOTION LAW PLOT FOR THE MOTOR IN PPS

CODE REMOVED FOR PUBLICATION PURPOSE
CONTACT marcozorzi@icloud.com FOR THE ORIGINAL CODE

%% REQUIRED TORQUE CALCULATION

CODE REMOVED FOR PUBLICATION PURPOSE
CONTACT marcozorzi@icloud.com FOR THE ORIGINAL CODE

%% REQUIRED TORQUE FIGURE

CODE REMOVED FOR PUBLICATION PURPOSE
CONTACT marcozorzi@icloud.com FOR THE ORIGINAL CODE

%% REQUIRED TORQUE AND PULLOUT CURVE VS SPEED

CODE REMOVED FOR PUBLICATION PURPOSE
CONTACT marcozorzi@icloud.com FOR THE ORIGINAL CODE

%% COMMUTATION PERIOD CALCULATION
```

CODE REMOVED FOR PUBLICATION PURPOSE
CONTACT marcozorzi@icloud.com FOR THE ORIGINAL CODE

```
%% SCREEN ORGANIZATION
scrsz = get(0,'ScreenSize');
scrx = scrsz(1,3);
scry = scrsz(1,4);
set(fig1,'Position', [0*(scrx/4) scry (scrx/4) ((scry/2)*0.75)]);
set(fig2,'Position', [1*(scrx/4) scry (scrx/4) ((scry/2)*0.75)]);
set(fig3,'Position', [2*(scrx/4) scry (scrx/4) ((scry/2)*0.75)]);
set(fig4,'Position', [3*(scrx/4) scry (scrx/4) ((scry/2)*0.75)]);
set(fig5,'Position', [0*(scrx/4) scry*0.08 (scrx/4) ((scry/2)*0.75)]);
set(fig6,'Position', [1*(scrx/4) scry*0.08 (scrx/4) ((scry/2)*0.75)]);
set(fig7,'Position', [2*(scrx/4) scry*0.08 (scrx/4) ((scry/2)*0.75)]);

display('-----HT34_v5 run succesfully-----')
```

APPENDIX B - MG0914 DATA ACQUISITION SYSTEM

In this appendix the data acquisition system of the MG0914 is presented. In order to monitor the car's working parameters and in order to analyse the car behaviour, the vehicle is equipped with a data acquisition system based on two motorsport products:

- Motec M400: an ECU (Engine Control Unit, Ed.) which controls the engine and senses its parameters through sensors.
- Motec ADL2: a Cockpit display which serves as data logger.

The ECU is able to temporarily log the sensor and, through a CAN Protocol (Controlled Area Network, Ed.), it is able to transfer every information to the ADL2, which logs these sensors. In addition, the ADL2 has various inputs itself and it can log directly sensors connected to it. All these informations can be sampled up to 1000 Hz and they are saved in a 16MB memory with 2 files. After that, these two files can be opened through Motec software, i2 Pro, which is vastly used in numerous motorsport environments. This software allows the user to make some calculations, filter data and put data and video side by side, for better understanding. An example of a data acquisition can be found in picture 58. In addition, if the user needs more advanced calculations, the software allows to export data both in .csv format and .mat format, which can be used in Microsoft Excel and Matlab.

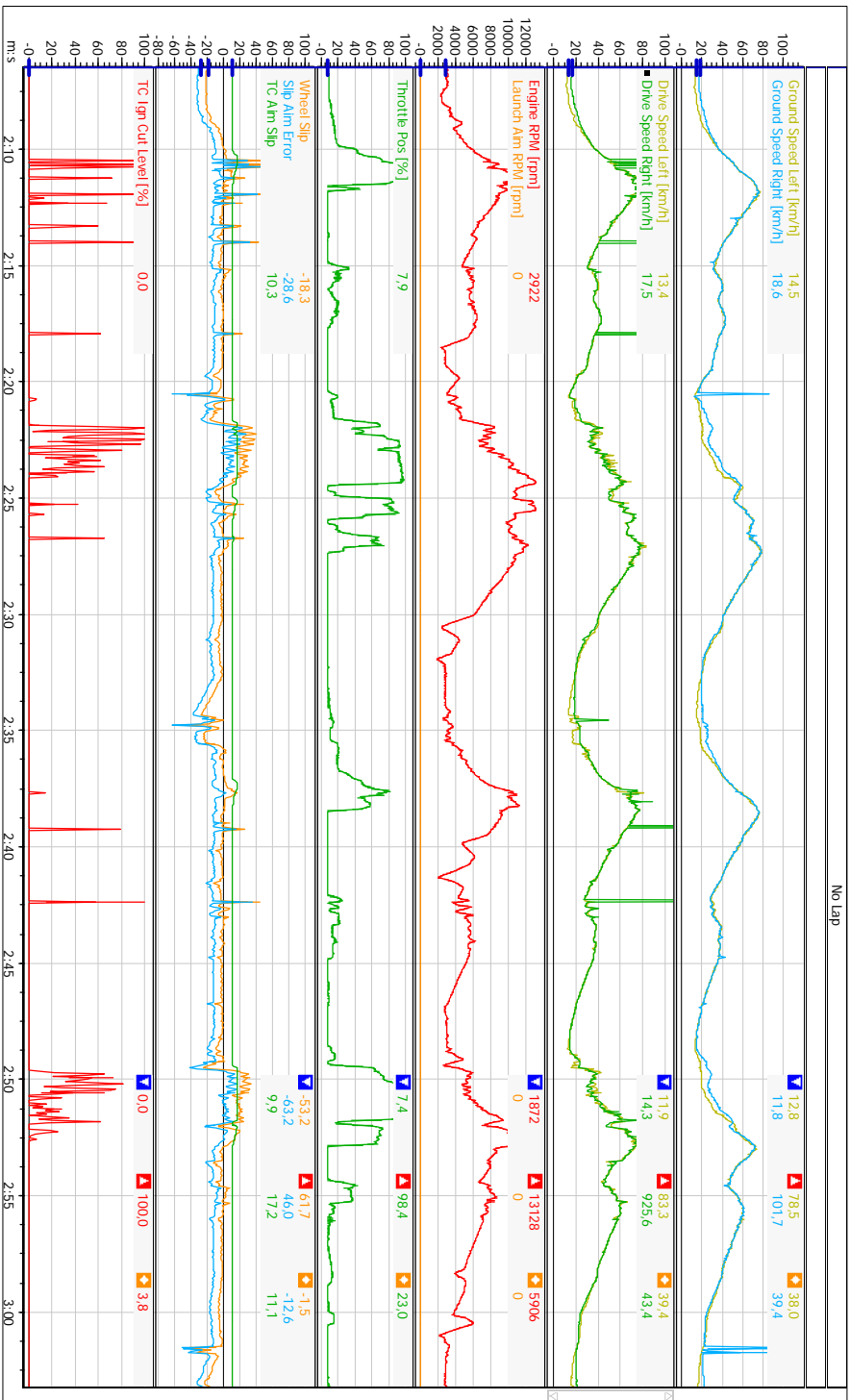


Figure 58: Example of iz Pro Data Acquisition software.

APPENDIX C - MATLAB® SCRIPT BLDCM RATIO

```

%%%%%%%%%%%%%%%%%%%%%%%%%%%%%%%%%%%%%%%%%%%%%%%%%%%%%%%%%%%%%%%%%%%%%%%%
% Brushless DC Motor Simulator %
%%%%%%%%%%%%%%%%%%%%%%%%%%%%%%%%%%%%%%%%%%%%%%%%%%%%%%%%%%%%%%%%%%%%%%%%

clc;
close all;
clear all;

%% VARIABLE INITIALIZATION
raccoltaDati();
load valori_precedenti.mat

[downshift_request, daq_time] = importDati(dati_acquisiti);
Jm = rotor_inertia*10^-3*10^-4;
Jv = gearbox_inertia*10^-7;
efficiency = eff/100;
working_temp = 55;
F = 270; % Force necessary to move the load. [N]
time_total = 0.25; % total time to move the load. [s]
time_rise = 0.2*time_total; % Time in which the load accelerates. [s]
movement_angle = 34; % degrees of engine clutch lever movement
movement_angle_rad = (movement_angle*pi)/180;
mean_angular_speed = movement_angle_rad / time_total;
radial_speed_peak = (mean_angular_speed*time_total)/(time_total-time_rise); %top
    radial speed reached by the motor [m/s]
C_th_winding = tau_winding/R_th_winding;
C_th_stator = tau_motor/R_th_stator;

s = tf('s');
Zc1 = 1/(s*C_th_winding);
Z2 = R_th_stator/(1+R_th_stator*C_th_stator*s);
W = (Zc1*R_th_winding+Zc1*Z2)/(Zc1+R_th_winding+Z2);

%% TIME DEFINITION
time = [0:0.001:time_total]; %Time vector
[uno, samples] = size(time); %Number of time units

%% DESIRED MOTION LAW
% In this section the calculation for the desired motion is implemented

CODE REMOVED FOR PUBLICATION PURPOSE
CONTACT marcorzori@icloud.com FOR THE ORIGINAL CODE

%% BEST RATIO LOOP

ratios = [250:50:1000];
temperature = zeros(1,size(ratios,2));
flag = 0;
ii = 1;
for ii = 1:size(ratios,2)
    TL = (F*0.037)/(ratios(ii)*efficiency);

    %% DESIRED MOTION LAW PLOT FOR THE MOTOR
    % The desired motion law is transferred to the motor through the ball screw

    CODE REMOVED FOR PUBLICATION PURPOSE
    CONTACT marcorzori@icloud.com FOR THE ORIGINAL CODE

    %% DESIRED MOTION LAW PLOT FOR THE MOTOR IN RPM
    % The desired motion law is transferred to the motor through the ball screw

    CODE REMOVED FOR PUBLICATION PURPOSE
    CONTACT marcorzori@icloud.com FOR THE ORIGINAL CODE

    %% REQUIRED TORQUE CALCULATION

    CODE REMOVED FOR PUBLICATION PURPOSE
    CONTACT marcorzori@icloud.com FOR THE ORIGINAL CODE

    %% REQUIRED CURRENT CALCULATION

    CODE REMOVED FOR PUBLICATION PURPOSE
    CONTACT marcorzori@icloud.com FOR THE ORIGINAL CODE

    %% POWER CALCULATION

    CODE REMOVED FOR PUBLICATION PURPOSE

```

```

CONTACT marcozorzi@icloud.com FOR THE ORIGINAL CODE

%% FINAL TEMPERATURE CALCULATION

CODE REMOVED FOR PUBLICATION PURPOSE
CONTACT marcozorzi@icloud.com FOR THE ORIGINAL CODE

%% PLOTS
CODE REMOVED FOR PUBLICATION PURPOSE
CONTACT marcozorzi@icloud.com FOR THE ORIGINAL CODE

%% SCREEN ORGANIZATION
scrsz = get(0, 'ScreenSize');
scrx = scrsz(1,3);
scry = scrsz(1,4);
set(fig1, 'Position', [0*(scrx/4) scry (scrx/4) ((scry/2)*0.75)]);
set(fig2, 'Position', [1*(scrx/4) scry (scrx/4) ((scry/2)*0.75)]);
set(fig3, 'Position', [2*(scrx/4) scry (scrx/4) ((scry/2)*0.75)]);
set(fig4, 'Position', [3*(scrx/4) scry (scrx/4) ((scry/2)*0.75)]);
set(fig5, 'Position', [0*(scrx/4) scry*0.08 (scrx/4) ((scry/2)*0.75)]);
set(fig6, 'Position', [1*(scrx/4) scry*0.08 (scrx/4) ((scry/2)*0.75)]);
set(fig7, 'Position', [2*(scrx/4) scry*0.08 (scrx/4) ((scry/2)*0.75)]);
set(fig8, 'Position', [3*(scrx/4) scry*0.08 (scrx/4) ((scry/2)*0.75)]);
set(fig9, 'Position', [0*(scrx/4)+(scrx/8) scry (scrx/4) ((scry/2)*0.75)]);
set(fig10, 'Position', [1*(scrx/4)+(scrx/8) scry (scrx/4) ((scry/2)*0.75)]);
set(fig11, 'Position', [2*(scrx/4)+(scrx/8) scry (scrx/4) ((scry/2)*0.75)]);

display('-----BIDCM SIMULATOR run succesfully-----')

```

APPENDIX D - MATLAB® SCRIPT BLDCM SIMULATION

```

%%%%%%%%%%%%%%%%%%%%%%%%%%%%%%%%%%%%%%%%%%%%%%%%%%%%%%%%%%%%%%%%%%%%%%%%
% Brushless DC Motor Simulator %
%%%%%%%%%%%%%%%%%%%%%%%%%%%%%%%%%%%%%%%%%%%%%%%%%%%%%%%%%%%%%%%%%%%%%%%%

clc;
close all;
clear all;

display('— Program started —')

%% INPUT DIALOG
val_def=load('valori_precedenti.mat');

input = {'Rotor Inertia[g*cm^2]:', 'Torque constant[mNm/A]', 'Gearbox Inertia[g*cm^2]: ', 'Efficiency [%]:', '
ratio:', 'Phase resistance (ohm):', 'R_th_rotor (KW):', 'R_th_winding (KW)', 'Rotor time constant (s)', '
Stator time constant (s)', 'DAQ file name (.mat)', 'Max winding temp'};
titolo = 'Motor Simulator';
numero_linee = 1;
valori_default1 = {num2str(val_def.rotor_inertia), num2str(val_def.Kt), num2str(val_def.gearbox_inertia),
num2str(val_def.eff), num2str(val_def.ratio), num2str(val_def.R_mot), num2str(val_def.R_th_winding),
num2str(val_def.R_th_stator), num2str(val_def.tau_winding), num2str(val_def.tau_motor), val_def.
dati_acquisiti, num2str(val_def.max_temp_motor)};

variabili = inputdlg(input, titolo, numero_linee, valori_default1);

rotor_inertia = str2double(variabili{1});
Kt = str2double(variabili{2});
gearbox_inertia = str2double(variabili{3});
eff = str2double(variabili{4});
ratio = str2double(variabili{5});
R_mot = str2double(variabili{6});
R_th_winding = str2double(variabili{7});
R_th_stator = str2double(variabili{8});
tau_winding = str2double(variabili{9});
tau_motor = str2double(variabili{10});
dati_acquisiti = variabili{11};
max_temp_motor = str2double(variabili{12});

display('— Saving started —')
save('valori_precedenti.mat');
display('— Saving ended —')

%% VARIABLE INITIALIZATION

% raccoltaDati();
% load valori_precedenti.mat

Jm = rotor_inertia*10^-3*10^-4;
Jv = gearbox_inertia*10^-7;
efficiency = eff/100;

working_temp = 55;
F = 270; % Force necessary to move the load. [N]
time_total = 0.25; % total time to move the load. [s]
time_rise = 0.2*time_total; % Time in which the load accelerates. [s]
movement_angle = 34; % degrees of engine clutch lever movement
movement_angle_rad = (movement_angle*pi)/180;
mean_angular_speed = movement_angle_rad / time_total;

radial_speed_peak = (mean_angular_speed*time_total)/(time_total-time_rise); %top
radial_speed_reached_by_the_motor [m/s]
TL = (F*0.037)/(ratio*efficiency); % Load Torque

%R_mot = R_mot*(1+0.0039*(working_temp-25));

time = [0:0.001:time_total]; %Time vector
[uno, samples] = size(time); %Number of time units

%% DESIRED MOTION LAW PLOT
% In this section the plot for the desired motion is implemented

CODE REMOVED FOR PUBLICATION PURPOSE
CONTACT marcozorzi@icloud.com FOR THE ORIGINAL CODE

```



```

%% DESIRED MOTION LAW PLOT FOR THE MOTOR
% The desired motion law is transferred to the motor through the ball screw

CODE REMOVED FOR PUBLICATION PURPOSE
CONTACT marcozorzi@icloud.com FOR THE ORIGINAL CODE

%% DESIRED MOTION LAW PLOT FOR THE MOTOR IN RPM
% The desired motion law is transferred to the motor through the ball screw

CODE REMOVED FOR PUBLICATION PURPOSE
CONTACT marcozorzi@icloud.com FOR THE ORIGINAL CODE

%% REQUIRED TORQUE CALCULATION

CODE REMOVED FOR PUBLICATION PURPOSE
CONTACT marcozorzi@icloud.com FOR THE ORIGINAL CODE

%% REQUIRED CURRENT CALCULATION

CODE REMOVED FOR PUBLICATION PURPOSE
CONTACT marcozorzi@icloud.com FOR THE ORIGINAL CODE

%% THERMAL CALCULATIONS

CODE REMOVED FOR PUBLICATION PURPOSE
CONTACT marcozorzi@icloud.com FOR THE ORIGINAL CODE

%% TRANSFER FUNCTION METHOD

CODE REMOVED FOR PUBLICATION PURPOSE
CONTACT marcozorzi@icloud.com FOR THE ORIGINAL CODE

%% CALCOLO FINALE TEMPERATURA

CODE REMOVED FOR PUBLICATION PURPOSE
CONTACT marcozorzi@icloud.com FOR THE ORIGINAL CODE

%% PLOTS

CODE REMOVED FOR PUBLICATION PURPOSE
CONTACT marcozorzi@icloud.com FOR THE ORIGINAL CODE

%% SCREEN ORGANIZATION
scrsz = get(0,'ScreenSize');
scrx = scrsz(1,3);
scry = scrsz(1,4);
set(fig1,'Position', [0*(scrx/4) scry (scrx/4) ((scry/2)*0.75)]);
set(fig2,'Position', [1*(scrx/4) scry (scrx/4) ((scry/2)*0.75)]);
set(fig3,'Position', [2*(scrx/4) scry (scrx/4) ((scry/2)*0.75)]);
set(fig4,'Position', [3*(scrx/4) scry (scrx/4) ((scry/2)*0.75)]);
set(fig5,'Position', [0*(scrx/4) scry*0.08 (scrx/4) ((scry/2)*0.75)]);
set(fig6,'Position', [1*(scrx/4) scry*0.08 (scrx/4) ((scry/2)*0.75)]);
set(fig7,'Position', [2*(scrx/4) scry*0.08 (scrx/4) ((scry/2)*0.75)]);
set(fig8,'Position', [3*(scrx/4) scry*0.08 (scrx/4) ((scry/2)*0.75)]);
set(fig9,'Position', [0*(scrx/4)+(scrx/8) scry (scrx/4) ((scry/2)*0.75)]);
set(fig10,'Position', [1*(scrx/4)+(scrx/8) scry (scrx/4) ((scry/2)*0.75)]);
set(fig11,'Position', [2*(scrx/4)+(scrx/8) scry (scrx/4) ((scry/2)*0.75)]);

display('-----BDCM SIMULATOR run succesfully-----')

```

BIBLIOGRAPHY

- [1] Maxon Academy. *Formulae handbook*. Sachelsen, 2012.
- [2] Paul Acarnley. *Stepping Motors - A Guide to Theory and Practice*. The Institution of Engineering and Technology, 2007.
- [3] SAE International. 2014 formula sae® rules - table of contents. 2014.
- [4] Mauro Zigliotto. *Fondamenti di Macchine e Azionamenti Elettrici*. Mauro Zigliotto, 2009.